

UC Berkeley

Research Reports

Title

Red-Light-Running Collision Avoidance: Final Report

Permalink

<https://escholarship.org/uc/item/55v7n1qr>

Authors

Grembek, Offer

Zhou, Kun

Li, Irene

et al.

Publication Date

2009

CALIFORNIA PATH PROGRAM
INSTITUTE OF TRANSPORTATION STUDIES
UNIVERSITY OF CALIFORNIA, BERKELEY

Red-Light-Running Collision Avoidance: Final Report

**Offer Grembek, Kun Zhou, Irene Li,
Meng Li, Wei-Bin Zhang**

**California PATH Research Report
UCB-ITS-PRR-2009-1**

This work was performed as part of the California PATH Program of the University of California, in cooperation with the State of California Business, Transportation, and Housing Agency, Department of Transportation, and the United States Department of Transportation, Federal Highway Administration.

The contents of this report reflect the views of the authors who are responsible for the facts and the accuracy of the data presented herein. The contents do not necessarily reflect the official views or policies of the State of California. This report does not constitute a standard, specification, or regulation.

Final Report for Task Order 6210

January 2009

ISSN 1055-1425

Red-Light-Running Collision Avoidance: Final Report

**Offer Grembek, Kun Zhou, Zhijun Zou, Wei-Bin Zhang
Irene Li and Meng Li**

Task Order: 6210

ACKNOWLEDGEMENTS

This work was performed by the California PATH Program at the University of California at Berkeley in cooperation with the State of California Business, Transportation and Housing Agency, Department of Transportation (Caltrans). The contents of this report reflect the views of the authors, who are responsible for the facts and the accuracy of the data presented herein. The contents do not necessarily reflect the official views or policies of the State of California.

The authors thank Greg Larson of Caltrans' Division of Research and Innovation, Kai Leung at Caltrans Headquarters, Paul Chiu and James Lau of Caltrans District 4, Professor Samer Madanat and Professor Alexander Skabardonis of Institute of Transportation Studies at UC Berkeley, Dr. Yafeng Yin (formerly at PATH) and Dr. Liping Zhang for their support and contributions.

ABSTRACT

Red-Light-Running (RLR) is the leading cause of urban crashes. This report presents the findings from an investigation of signal control-related countermeasures to reduce the occurrences of RLR and related collisions. The objectives of this study were to identify and evaluate potential modifications to signal timing schemes in reducing the frequency of RLR and to develop online adaptive RLR collision avoidance algorithms to reduce the possibility of RLR collisions. High quality, second-by-second vehicle count and signal timing and phasing data were collected at arterial intersections. A signal-cycle-based data analysis was performed to determine RLR contributing factors that are statistically significant, having substantial impact on RLR and controllable via signal timing modifications. These findings were then applied to develop signal timing schemes that aim to increase the probability of stopping and online signal timing adaptation strategies to avoid potential collision when RLR occurs. We demonstrate the effectiveness of signal timing modifications in reducing RLR while maintaining intersections' level of service, under both microscopic simulation and macroscopic simulation environments. In addition, an investigation of drivers' decision making at signalized intersections using real world data and a probabilistic RLR prediction model are presented.

Key Words: red-light running, collision avoidance, signal timing modification, safety

EXECUTIVE SUMMARY

Red-light-running (RLR) is the leading cause of urban crashes. In the United States RLR causes more than 200,000 crashes annually. These crashes led to 940 deaths and 188,000 injuries. Red-light-running collision avoidance systems can help save lives by preventing these crashes.

This research study is a cooperative effort between California PATH program at UC Berkeley and California Department of Transportation (Caltrans). The objectives of this study are two-fold: 1) to identify and evaluate potential modifications to signal timing schemes so that they will improve intersection safety, and 2) to develop “adaptive” RLR collision avoidance algorithms which are able to react to the predicted RLR collision in real-time.

The primary step for RLR collision avoidance is to understand how traffic operation factors (i.e., traffic flow, signal timing, etc) contribute to the occurrence of RLR. Although many studies have investigated the effects of traffic flow and signal timing factors on RLR, there is still much to be learned. RLR occurs in a relatively small time-space period, more specifically, the signal phase transition period. Meaningful analysis of RLR behaviors requires detailed data of that relevant period. The most often studied traffic flow parameter is the average daily traffic (ADT), which is, at best, aggregated over five-minute intervals and covers several signal cycles. This type of aggregated data can reveal important factors associated with RLR.

However, the data rarely possess the level of details needed for the in-depth analysis that is required for RLR collision avoidance.

Under a couple of PATH projects, a data acquisition system (DAS) was implemented to collect second-by-second signal phasing and timing data and traffic data (loop count and occupancy) at arterial intersections. The high resolution data make it possible to conduct cycle-based RLR study that can isolate the relevant traffic operations factors.

Using collected second-by-second data, logistic regression analysis was applied to estimate contributing factors to RLR. The departure loops at stop-line serve as the detection of RLR incidences, and the advance loops, which are 60 meters upstream from the stop-line (4 seconds travel time to the stop-line under posted speed limit of 35 mph), are used to capture the contributing factors. The in-use yellow duration and all-red clearance duration were compared with the values recommended by the Institute of Transportation Engineers (ITE) to justify the change interval is appropriately designed. The sensitivity of each loop detector was manual calibrated to ensure the accuracy of vehicle counts. For the cycle-based analysis, the data set collected during every signal cycle represents a sample, and each sample has data for the green, yellow and red signal phases for evaluating the impact of the different phases of the traffic signal. The analysis shows that average traffic flow clearly has an effect on RLR; however, the yellow arrival flow (i.e., the number of vehicles arrived at advance loops during the yellow signal phase) is shown to be the most significant and has the highest impact on RLR probability. This demonstrates how the use of detailed data can reveal information which

might be difficult to uncover when aggregated data is used. More significantly, since the yellow arrival flow is controllable through signal timing modifications such as adjusting the signal offsets, this finding suggests that yellow arrival flow can be used as a safety measure in the design of signal timing and that signal timing modification strategies that terminate the green phase based on the patterns of arrival flow can reduce the yellow arrivals and consequently reduce RLR probability and related collisions.

A TRANSYT-7F simulation model was constructed to study the effect of adjusting signal offsets on yellow arrival flow as well as traffic intersection delay. It is shown that the reduction of yellow arrival flow is indeed achievable while the intersection delay is preserved. We then developed an safety enhanced signal offsets optimization model which takes the yellow arrival flow into consideration and makes the best tradeoff between intersection efficiency (i.e., the intersection delay) and intersection safety (i.e., the probability of RLR).

A macroscopic simulation network (TRANSYT-7F) and a microscopic simulation network (VISSIM) were built to evaluate the effectiveness of the enhanced signal offsets optimization algorithm. The simulation networks were calibrated using field observation data (vehicle counts and turning ratios) to mimic the operation of a 6-intersection arterial network in Palo Alto, CA. The measures of effectiveness (MOEs) include the yellow arrival flow, the intersection delay, the number of stops and traffic progression. MOEs with current in-use offsets were compared with that obtained from modified offsets. TRANSYT-7F simulation and VISSIM simulation show a similar trend and both present very positive results:

- Yellow arrival flow was reduced significantly, by about 50%;
- Intersection delay was reduced by 4.9% (TRANSYT-7F) and by 2.5% (VISSIM);
- Number of stops increased by 2.3%; and
- Traffic progression dropped by 0.3%.

The simulation study demonstrates that there is still room for improving traffic safety within the existing traffic operations models without compromising intersection efficiency, and the offsets optimization model developed under this project showed it's capability in achieving this goal.

A nature extension of safety enhanced offsets optimization is to add the functionality of adaptive offsets to changes of traffic patterns. Our feasibility simulation study demonstrates the potential of such adaptivity in achieving more significant safety benefits.

In addition to traffic flow and signal control factors, driver's decision making during the signal transition period also contributes to RLR behaviors and related crashes. From the empirical data, we found that the majority of decisions were made during the first 2 seconds of yellow phase and drivers seem not change their decision in the last two seconds of yellow. An empirical-data-based probabilistic RLR prediction model is then developed and serves as the foundation to derive a dynamic yellow onset model, which determines the "best" point to terminate the green phase in the sense of minimizing the probability of RLR collision.

TABLE OF CONTENTS

ACKNOWLEDGEMENTS	I
ABSTRACT	I
EXECUTIVE SUMMARY	II
TABLE OF CONTENTS	VII
TABLE OF FIGURES	IX
1 BACKGROUND AND OVERVIEW	1
1.1 BACKGROUND	1
1.1.1 <i>Human Factors</i>	1
1.1.2 <i>Intersection Characteristics</i>	2
1.1.3 <i>Policy and Regulatory Factors</i>	4
1.2 PROJECT OVERVIEW	4
1.2.1 <i>Development of Signal Timing Schemes to Improve Intersection Safety</i>	5
1.2.2 <i>Development of Active RLR Collision Avoidance Countermeasures</i>	6
1.3 REFERENCES	6
2 STUDY ON RED-LIGHT RUNNING FACTORS	8
2.1 MOTIVATION	8
2.2 DATA COLLECTION.....	10
2.2.1 <i>Data Acquisition System</i>	10
2.2.2 <i>Study Site Selection</i>	11
2.2.3 <i>Site Description</i>	11
2.2.4 <i>Yellow Duration and Red-Clearance Duration</i>	13
2.2.5 <i>Collected Data</i>	14
2.3 RED-LIGHT-RUNNING STATISTICS.....	14
2.3.1 <i>Frequency of Red-Light-Running</i>	14
2.3.2 <i>Red-Light-Running Frequency versus Approach Flow Rate</i>	18
2.4 CYCLE-BASED DATA ANALYSIS.....	20
2.4.1 <i>Data Preparation and Processing</i>	20
2.4.2 <i>Statistical Analysis Method</i>	22
2.4.3 <i>Results of Regression Analysis</i>	24
2.4.4 <i>Impacts of Significant Variables</i>	26
2.4.5 <i>Focusing on Yellow Arrival Flow</i>	27
2.5 DISCUSSION	28
2.6 REFERENCES	30
3 DEVELOPMENT OF A SAFETY ENHANCED SIGNAL TIMING OPTIMIZATION MODEL	32
3.1 MOTIVATION	32
3.2 FEASIBILITY STUDY	33
3.2.1 <i>TRANSYT -7F Simulation Model</i>	34
3.2.2 <i>Results for Isolated Intersections</i>	36
3.2.3 <i>Results for the Corridor</i>	41
3.3 THE OPTIMIZATION MODEL.....	43
3.3.1 <i>Formulating the Optimization Problem</i>	43
3.3.2 <i>The Optimization Process</i>	44

3.3.3	<i>Comparing to a Genetic Algorithm</i>	46
3.4	THE OPTIMIZATION TOOL PACKAGE	46
3.4.1	<i>The Optimization Core</i>	47
3.4.2	<i>The TRANSYT-7F Model</i>	47
3.4.3	<i>The Batch Inserter</i>	48
3.4.4	<i>The MOE Extractor</i>	48
3.4.5	<i>The User Interface</i>	48
3.5	CONSIDERATIONS ON THE WEIGHT.....	50
3.6	REFERENCES	53
4	SIMULATION EVALUATION	54
4.1	INTRODUCTION	54
4.2	THE STUDY ARTERIAL CORRIDOR	54
4.3	OPTIMIZATION OF OFFSETS	55
4.3.1	<i>The Selection of Weight</i>	55
4.3.2	<i>The Optimization Process and Results</i>	57
4.3.3	<i>Comparison of Green Band</i>	59
4.3.4	<i>Analysis for Individual Intersections</i>	61
4.4	SIMULATION VALIDATION USING VISSIM	63
4.4.1	<i>The Simulation Model</i>	63
4.4.2	<i>VISSIM Network Building</i>	63
4.4.3	<i>Origin-Destination (OD) Matrix</i>	65
4.4.4	<i>MOE Collection</i>	65
4.4.5	<i>Simulation Results</i>	66
4.5	REFERENCES	69
5	ACTIVE RED-LIGHT-RUNNING COLLISION AVOIDANCE COUNTERMEASURES	70
5.1	INTRODUCTION	70
5.2	ACTIVE OFFSETS REFINING	73
5.3	DYNAMIC YELLOW ONSET	75
5.4	DYNAMIC RED CLEARANCE INTERVAL	78
5.5	REFERENCES	80
6	STUDY DRIVERS DECISION MAKING AT SIGNALIZED INTERSECTIONS	82
6.1	INTRODUCTION	82
6.2	DATA COLLECTION.....	83
6.3	DATA ASSOCIATION TO RECONSTRUCT VEHICLE TRAJECTORIES.....	85
6.4	PREDICTION OF RED-LIGHT RUNNING	88
6.5	DRIVERS' SITUATION ZONES	91
6.6	REFERENCES	94
7	CONCLUSIONS AND NEXT STEPS	95

TABLE OF FIGURES

FIGURE 2-1 ARCHITECTURE OF THE DATA ACQUISITION SYSTEM.....	10
FIGURE 2-2 AERIAL PHOTO OF EL CAMINO REAL AT 28 TH AVENUE	12
FIGURE 2-3 APPROACH FLOW RATE AS FUNCTION OF TIME-OF-DAY.....	15
FIGURE 2-4 RLR OCCURRENCES PER HOUR AS FUNCTION OF TIME-OF-DAY.....	17
FIGURE 2-5 RLR OCCURRENCES PER 1,000 ENTERING VEHICLES AS FUNCTION OF TIME-OF-DAY	17
FIGURE 2-6 RLR FREQUENCY VS. APPROACH FLOW RATE (SOUTHBOUND, 7 AM - 10 AM)	18
FIGURE 2-7 RLR FREQUENCY VS. APPROACH FLOW RATE (SOUTHBOUND, 4 PM - 8 PM)	19
FIGURE 3-1 AERIAL PHOTO OF STUDY SITE.....	35
FIGURE 3-2 DELAY AND YELLOW ARRIVALS AS A FUNCTION OF OFFSET	36
FIGURE 3-3 DELAY AND YELLOW ARRIVALS WITH TIME-SPACE DIAGRAMS.....	38
FIGURE 3-4 DELAY AND YELLOW ARRIVAL DIAGRAM FOR SPECIFIC LINKS.....	40
FIGURE 3-5 DELAY AND YELLOW ARRIVAL DIAGRAMS FOR THE CORRIDOR.....	42
FIGURE 3-6 FLOW CHART OF THE OPTIMIZATION ALGORITHM	45
FIGURE 3-7 ARCHITECTURE OF THE OPTIMIZATION TOOL.....	47
FIGURE 3-8 USER INTERFACE – MAIN WINDOW	49
FIGURE 3-9 USER INTERFACE – GRAPHIC WINDOW.....	50
FIGURE 3-10 YELLOW ARRIVAL FLOW AND DELAY AS FUNCTIONS OF WEIGHT.....	51
FIGURE 3-11 PROGRESSION AND NUMBER OF STOPS AS FUNCTIONS OF WEIGHT.....	52
FIGURE 4-1 AERIAL PHOTO OF THE STUDY SITE.....	55
FIGURE 4-2 MOES AS FUNCTIONS OF WEIGHTS	56
FIGURE 4-3 OPTIMIZATION RESULTS	58
FIGURE 4-4 COMPARISON OF GREEN BAND	60
FIGURE 4-5 COMPARISON OF YELLOW ARRIVAL FLOW FOR INDIVIDUAL INTERSECTIONS.....	61
FIGURE 4-6 COMPARISON OF DELAY FOR INDIVIDUAL INTERSECTIONS	62
FIGURE 4-7 AN INTERSECTION LAYOUT IN VISSIM WITH REAL-WORLD BACKGROUND	64
FIGURE 4-8 A BIRD’S-EYE VIEW OF THE STUDY CORRIDOR STRETCH IN VISSIM	64
FIGURE 4-9 COLLECTION OF MEASURES OF EFFECTIVENESS IN VISSIM	66
FIGURE 4-10 FLOW PER LINK FOR THE CURRENT OFFSETS.....	67
FIGURE 4-11 DELAY PER LINK FOR THE CURRENT OFFSETS.....	68
FIGURE 5-1 DILEMMA ZONE (TAKEN FROM [5-4])	71
FIGURE 5-2 DISTANCE TO STOPLINE – SPEED DIAGRAM OF DILEMMA ZONE (TAKEN FROM [5-4])	72
FIGURE 5-3 EVALUATION OF THE ACTIVE OFFSETS REFINING APPROACH	75
FIGURE 5-4 RED-LIGHT VIOLATION FREQUENCY VERSUS VIOLATION TIME INTO RED.....	78
FIGURE 6-1 DIFFERENT CHARACTERISTICS OF STOPPING AND THROUGH VEHICLES.....	82
FIGURE 6-2 DATA COLLECTION SITE	84
FIGURE 6-3 RECONSTRUCTED VEHICLE TRAJECTORIES.....	86
FIGURE 6-4 RLR FREQUENCY VERSUS ENTERING TIME INTO RED.....	87
FIGURE 6-5 STOPPING PROBABILITY VERSUS TRAVEL TIME TO THE STOPLINE	88
FIGURE 6-6 CORRECT RLR PREDICTION RATES	90
FIGURE 6-7 DRIVERS’ SITUATION ZONE WITH A YELLOW INDICATION	91

1 BACKGROUND AND OVERVIEW

1.1 Background

Red-light-running (RLR) is defined as a vehicle entering and proceeding through a signalized intersection after the traffic signal has turned red. RLR violation is reported to be increasing and has become a major national safety problem. Based on data provided by the Federal Highway Administration (FHWA), there were about 218,000 RLR crashes in Year 2001, resulting in as many as 181,000 injuries and 880 fatalities. The annual economic loss resulting from these incidents is estimated to be \$14 billion ([1-1]). In the city and county of San Francisco, California, RLR collisions cost the economy \$40 million each year not including property damage costs ([1-2]).

RLR is influenced by a variety of factors, including driver behavioral factors (human factors), intersection characteristics, policy and regulatory factors.

1.1.1 Human Factors

No specific category of red-light runners has been identified. However, the most frequent violators are likely to be young, and have previous traffic convictions and are usually alone in the car ([1-3]). Studies have also shown that being in a rush typically results in drivers taking higher risks. According to a FWHA survey [1-4], 48% of red light runners said they ran lights because they were in a hurry.

Many researchers have investigated drivers' decision-making processes at signalized intersections. The probability of a driver stopping in response to the onset of a yellow indication was discussed in a variety of literature. For instance, a study by Olson and Rothery ([1-5]) indicates that a driver's probability of stopping is based on the speed and distance to the stop line, the driver's perception of his/her ability to stop and the degree of comfort associated with the stop.

1.1.2 *Intersection Characteristics*

Three major categories of environmental factors were studied in past studies: traffic flow, intersection geometry and signal visibility, and signal timing.

1.1.2.1 Traffic Flow

The most often studied parameter in the traffic flow category is average daily traffic (ADT). Several studies have shown that increased ADT on the through direction increases RLR and that increased ADT on the crossing approaches increases the probability for collision (e.g., [1-6], [1-7]). Kamyab *et al.* ([1-8]) reported the relationship between the occurrence of RLR and traffic flow rates based on 1,242 hours of observation at 12 intersections in Iowa. Their results indicate that RLR increases at a rate of about 3.0 violations per 1,000 vehicles per hour in urban areas.

1.1.2.2 Intersection Geometry and Signal Visibility

Studies have shown that every additional lane on the main approach to an intersection increases the probability of a vehicle running the red light on a minor street by 7% ([1-6]). The

grade of an intersection approach affects drivers' probability of stopping. Drivers on downgrades are less likely to stop than drivers on level or upgrade approaches (at a given travel time to the stopline) ([1-11]). Poor signal visibility could also affect the RLR rate. According to a survey study ([1-1]), 40 percent of red-light violators claimed that they did not see the signal or its indication. Although it is not likely that all the claims are true, there probably are situations where a more visible signal would not have been violated.

1.1.2.3 Signal Timing

Signal timing is also a frequently studied factor in RLR research. Studies have shown that increased all-red intervals increase RLR while not necessarily increasing RLR collisions ([1-9]). In addition, researchers have found that the violation frequency is positively correlated with the frequency of yellow-signal presentation (i.e., how often the yellow signal appears within a period of time) ([1-10]). It has also been found that long cycle length reduces RLR ([1-11]). Van der Horst and Wilpink ([1-12]) showed that yellow and all-red intervals have a direct effect on the frequency of RLR -- they suggest that setting the yellow interval longer than 3.5 seconds is of great significance in reducing RLR frequency and that setting all-red intervals close to values proposed by the Institute of Transportation Engineering (ITE) can reduce violation rates and potential right-angle conflicts.

Van der Horst and Wilpink ([1-12]) reported that drivers approaching an actuated intersection are less likely to stop than if they are approaching a fixed-timing intersection. This finding suggests that drivers learn which signals are actuated and then develop an expectation of

service as they travel through the detection zone. The authors extrapolated this finding to drivers traveling within platoons through a series of coordinated signals. Drivers in a platoon seem to have an expectation that they can travel without interruption through successive signals. Their expectancy is that each signal they approach will remain green until after they pass through the intersection. Their desire to stay within the platoon makes them less willing to stop at the onset of the yellow indication.

1.1.3 Policy and Regulatory Factors

Policy and regulatory factors include legislation and education programs that aim to reduce RLR. Red-light photo enforcement has been shown to reduce RLR by 23 to 70 percent and RLR collisions by 22 to 40 percent ([1-10]). Regarding legislation, it has been shown that compliance with the ITE formulation for calculating the yellow interval can reduce the RLR frequency ([1-8]).

1.2 Project Overview

The objectives of this project are two-fold: (1) to identify and evaluate potential modifications to signal timing schemes so that they will improve intersection safety, and (2) to develop an “adaptive” red-light running collision avoidance algorithm which is able to react to the predicted RLR collision in real-time. Both objectives require significant data collection and analysis along with identifying the detection, hardware/software, and communication requirements that will lead to the development and implementation of a field testing system.

1.2.1 Development of Signal Timing Schemes to Improve Intersection Safety

The development of a RLR collision avoidance system requires a comprehensive understanding of factors contributing to RLR. The challenges of this development are primarily associated with learning what RLR related factors can be used to incorporate safety considerations in timing plans and how they influence the efficiency of traffic signal system control.

We performed a comprehensive cycle-based RLR data analysis using detailed second-by-second traffic volume and traffic signal status data. Through the data analysis, it was found that the flow that arrived at the advance loops during the yellow phase, defined in this study as yellow arrival flow, has the largest impact on RLR frequency and could be a potential safety measure.

Considering the yellow arrival flow as a controllable parameter, an optimization algorithm was developed to fine-tune the signal offsets in order to reduce the probability of RLR without compromising operational efficiency, or overall system delay. We can demonstrate the effectiveness of the proposed algorithm through both microscopic and macroscopic traffic simulation. A user-friendly simulation tool package has also been developed for traffic engineers.

1.2.2 Development of Active RLR Collision Avoidance Countermeasures

Three active countermeasures were proposed, including an offset adjustment that adapts to traffic demand, a dynamic yellow onset that adapts to traffic arrival patterns and a dynamic red clearance interval that adapts to the predicted probability of RLR. Logistic regression was performed based on empirical data to understand drivers' stop-or-go decisions at an intersection and to develop a RLR prediction model.

The rest of this report is organized as follows. Chapter 2 presents the methodologies and findings for the analysis of contributing factors for RLR. The offset optimization algorithm and the optimization tool are presented in Chapter 3. The effectiveness evaluation of the algorithm through simulation is reported in Chapter 4. Chapter 5 presents discussions on active RLR collision avoidance countermeasures. The studies of drivers' decision making at an intersection and the RLR prediction model are discussed on Chapter 6. Chapter 7 provides conclusions and next research steps.

1.3 References

- [1-1] *Make Intersections Safer: A Toolbox of Engineering Countermeasures to Reduce Red-Light-Running*. Washington DC: Federal Highway Administration. 2003.
- [1-2] *San Francisco 2003 Collision Report*. City and County of San Francisco, Department of Parking and Transportation. November, 2004.
- [1-3] Retting, R. A. and Williams A.F., Characteristics of Red Light Violators: Results of a Field Investigation. *Journal of Safety Research*. Vol. 27, 1996.

- [1-4] *Stop Red Light Running Facts*. Federal Highway Administration.
http://safety.fhwa.dot.gov/fourthlevel/pro_res_srlr_facts.htm
- [1-5] Olson, P. L. and Rothery, R. W., Driver Response to the Amber Phase of Traffic Signals. *Traffic Engineering*, Institute of Traffic Engineers, Washington, D.C., February 1962.
- [1-6] Mohamedshah, Y., Chen, L., and Council, F., Association of Selected Intersection Factors with Red Light Running Crashes. *Conference Proceedings of the Institute of Transportation Engineers Annual Meeting*. 2000.
- [1-7] Bonneson, J.A., Middleton, D., Zimmerman, K., Charara, H. and Abbas, M., *Intelligent Detection-Control System for Rural Signalized Intersections*. Report No. FHWA/TX-02/4022-2. Texas Department of Transportation, Austin, Texas, August 2002.
- [1-8] Kamyab, A., McDonald, T., Stribiak, J., Storm, B. and Anderson-Wilk, M., *Red Light Running in Iowa: The Scope, Impact, and Possible Implications*. Center for Transportation Research and Education. Ames, IA, December 2000.
- [1-9] Retting, R. A. and Greene, M. A., Influence of Traffic Signal Timing on Red-Light Running and Potential Vehicle Conflicts at Urban Intersections. *Transportation Research Record: Journal of the Transportation Research Board*, No. 1595, TRB, National Research Council, Washington, D.C., 1997.
- [1-10] Ruby, D.E. and Hobeika, A. G., Assessment of Red Light Running Cameras in Fairfax County, Virginia. In *Proceedings of Transportation Research Board Annual Meeting*. Transportation Research Board, Washington, D.C., 2003.
- [1-11] Bonneson, J, Zimmerman, K., and Brewer, M., *Engineering Countermeasures to Reduce Red-Light Running*. Report FHWA/TX-03/4027-2, Washington DC: Federal Highway Administration, 2003.
- [1-12] Van der Horst, R. and Wilmink, A., Driver's Decision-Making at Signalized Intersections: An Optimization of the Yellow Timing. *Traffic Engineering & Control*. 1986.

2 STUDY ON RED-LIGHT RUNNING FACTORS

2.1 Motivation

The phenomenon of Red-Light-Running (RLR) is influenced by a variety of factors. Some of them are behavioral factors, which represent the choices made by individual drivers. Others are vehicle characteristic factors and traffic operation factors (such as traffic flow and signal timing) which contribute to RLR occurrences. This analysis will focus on traffic operation factors, partially because of the scarce data and information related to behavioral factors and primarily because traffic operation factors provide a likely set of countermeasures.

Many studies have investigated the effect of traffic flow on RLR. The most often studied parameter is average daily traffic (ADT). Several studies have shown that increased ADT on the subject approach increases RLR and that increased ADT on the cross approach increases the probability of collision (e.g. [2-1] and [2-2]). Kamyab *et al.* ([2-4]) reported the relationship between the frequency of RLR and traffic flow rates based on 1,242 hours of observation over 12 intersections in Iowa. Their results indicate that RLR increases at a rate of about 3.0 RLR occurrences per 1,000 entering vehicles in urban areas.

The risk for RLR is not constant within a traffic signal cycle. The risk is highest when drivers approach the intersection during the signal phase transition and the risk is zero when vehicles approach the intersection during the green phase. Since red-light violations occur in a

relatively small time-space period, meaningful analysis of RLR requires detailed data of that relevant period. The data regularly collected by traffic agencies is, at best, aggregated over five-minute intervals, covering several signal cycles and can reveal important factors associated with RLR, such as ADT. However, this data rarely possess the level of detail needed for the in-depth analysis that is required to study RLR issues and to develop advanced intersection safety measures.

Within a couple of PATH projects that conducted development and field testing of an Adaptive Transit Signal Priority (ATSP) system, a data acquisition system (DAS) was implemented to collect second-by-second traffic signal status data (phase and interval) and traffic data (loop count and occupancy) from local signal controllers ([2-6]). The detailed signal status and traffic data make it possible to conduct a cycle-based RLR study that can isolate the relevant traffic operations factors.

To obtain the practical benefits required from this type of study, the research team defined the desirable traits of the RLR factors so that they could be used to develop countermeasures. The factors contributing to RLR identified have to satisfy the following criteria:

- Statistical significance - Guarantee that the results are valid and reproducible.
- Controllable - Can be controlled by signal timing parameters for the purpose of countermeasure development.

- Substantial impact on RLR - Increase the chances that controlling these factors would change the probability of RLR since some factors can be highly significant but changing them would result in negligible changes in RLR probability.

2.2 Data Collection

2.2.1 Data Acquisition System

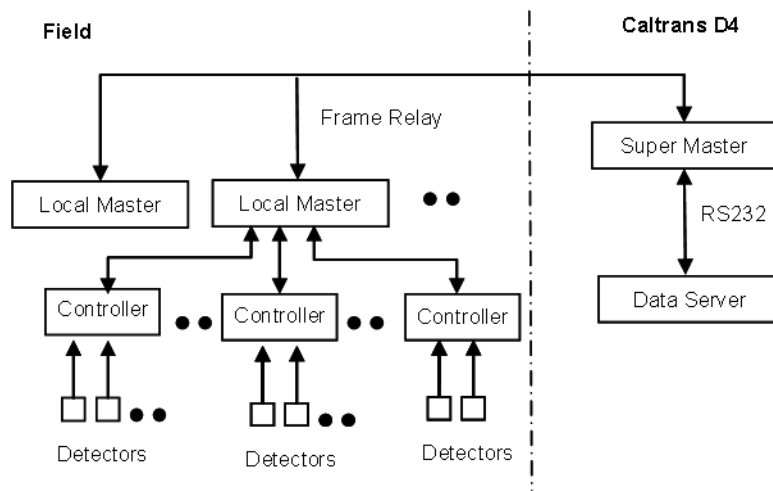


Figure 2-1 Architecture of the Data Acquisition System

Figure 2-1 illustrates the physical architecture of the data acquisition system (DAS). The DAS has been implemented on the El Camino Real corridor on California State Highway 82, in the city of San Mateo. The corridor consists of eight signalized intersections from the 9th Street to the 31st Avenue. The traffic control system for this corridor is operated under Caltrans C-8 Traffic Control software together with Model 170E traffic signal controllers. The system provides coordinated and semi-actuated operation.

The signal control system used along this corridor is a closed-loop system with control logic distributed among three levels: the local controller, the on-street master controller and the super master controller. Typically, the local controller receives information from loop detectors, the local master controller receives information from the local controllers and the super master enables the system operator to monitor and control the system's operation based on data collected from the field. The data available from the signal control system include time-of-day (TOD) timing plans, second-by-second traffic counts, occupancy and signal status. The data server hosts a real-time database and connects with the super master via serial port connection, allowing traffic data and signal status to be received by the real-time database.

2.2.2 Study Site Selection

In order to detect RLR incidence from the loop detector, departure loops at the stopline are required. Each of the eight intersections has advance loop detectors for the coordinated phases that control the vehicle movements along El Camino Real, but has no departure loops. Only the intersection at 28th Avenue has presence loop detectors and each detector consists of four inter-connected inductive loops. This intersection was selected as the study site. The loop closest to the stopline on each through lane was isolated from the presence loop detector to serve as the departure loop.

2.2.3 Site Description

The intersection of El Camino Real at 28th Avenue is a T-intersection. A satellite photo of this intersection is shown in Figure 2-2.

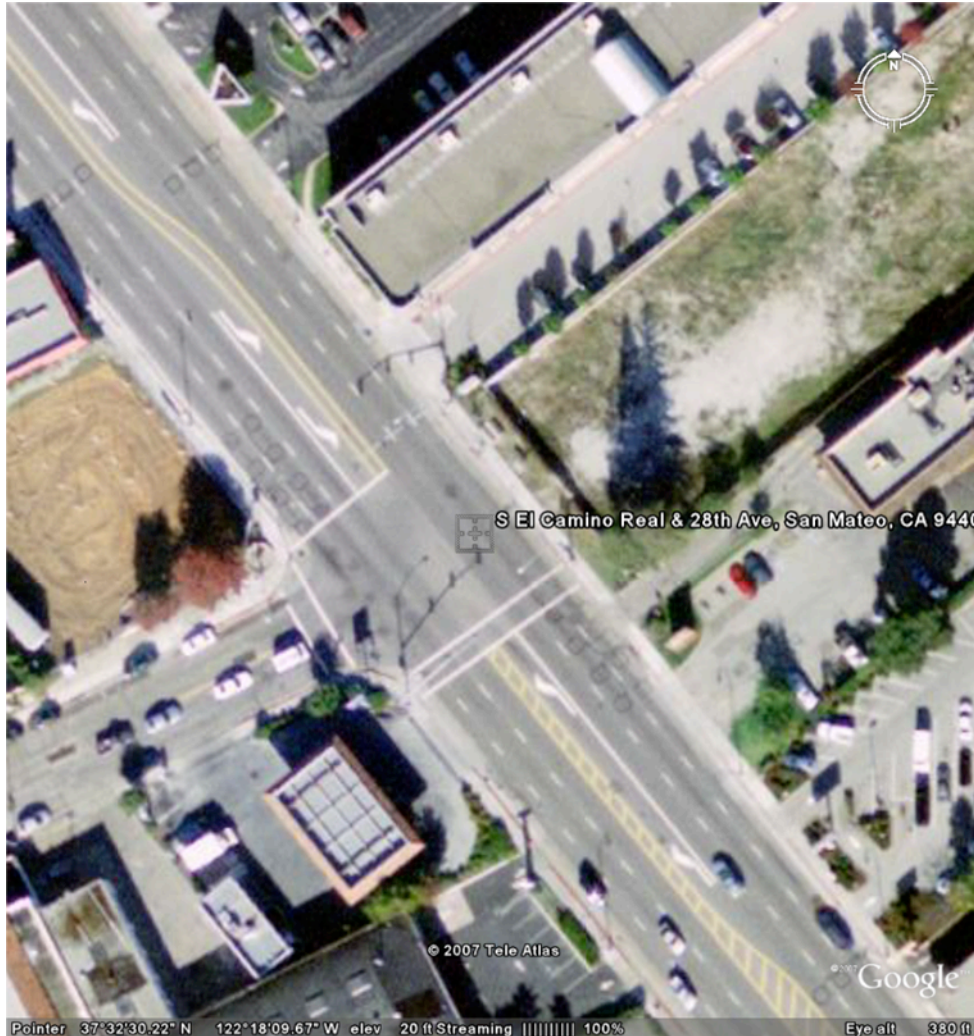


Figure 2-2 Aerial Photo of El Camino Real at 28th Avenue

There are three through lanes and one left-turn pocket on the northbound and southbound of El Camino Real. The through movements in the northbound direction are controlled by phase 6 and those on southbound by phase 2, respectively. The left-turn movements are protected. The

advance loops are 60 meters upstream from the stopline, which is about 4 seconds travel time to the stopline if a vehicle is traveling at the posted speed limit at 35MPH.

There are three time-of-day traffic control plans as shown in Table 2-1.

Table 2-1 Traffic Control Plans

Plan	Effective Time	Cycle Length (sec.)
1	7:00 – 10:00	90
2	10:00 – 15:30	100
3	15:30 – 20:00	110

2.2.4 *Yellow Duration and Red-Clearance Duration*

The Manual on Uniform Traffic Control Devices (MUTCD) ([2-8]) requires that a yellow-signal indication be displayed immediately following every green-signal indication to warn the motorists that the green-signal indication is being terminated and a red-signal indication will be exhibited immediately thereafter. Between the green indication and the red indication, the yellow interval and the red-clearance interval are also named the change interval. Inappropriate length of the change interval can cause driver confusion and result in RLR and collisions ([2-10]). It is essential to compare the change interval with the values recommended by the Institute of Transportation Engineers (ITE).

In the current edition of ITE's *Traffic Engineering Handbook* ([2-12]), the recommended change interval is calculated using the "ITE formula" as follows:

$$Y = \delta + \frac{V}{2a + 2Gg}$$

$$AR = \frac{W + L}{V}$$

Eq. 2-1

Where:

Y = yellow interval in seconds

AR = red - clearance interval in seconds

δ = driver perception - reaction time, typically 1 sec.

V = speed of approaching traffic in m/s, typically the posted speed limit

a = comfortable deceleration rate, typically 3 m/sec²

g = acceleration due to gravity, 9.8 m/sec²

G = grade of the intersection on approach in percent divided by 100

W = width of the intersection in m.

L = length of vehicle, typically 6 m

The ITE recommended yellow interval and red-clearance interval are 3.6 seconds and 1.8 seconds, respectively. The intervals in use at the intersection are 4 seconds and 1 second. The change interval is therefore designed appropriately for the intersection.

2.2.5 *Collected Data*

One month of data from October 2004 were collected at the study site. The data were collected 5 days per week, 8.5 hours per day between 7AM and 8PM when the signal was operated under coordination. The data, with one-second resolution, include vehicle count, vehicle occupancy and the corresponding signal status.

2.3 Red-Light-Running Statistics

2.3.1 Frequency of Red-Light-Running

The departure loops were used to capture the RLR occurrences. More specifically, the detection of a vehicle during the red phase on the subject approach indicates an occurrence of RLR. When traveling on the southbound direction, motorists can make a right-turn on red from the curb lane. In order to exclude those Right-Turn-On-Red movements, the traffic counts on this lane, including both the advance loop and departure loop, were excluded in this study.

Figure 2-3 shows the approach flow rate as a function of time-of-day, for both the southbound and northbound traffic. The flow rate is measured at the advance loops. The average flow rate on the northbound is about 379 VPH (vehicles per hour) per lane, and the average flow on the southbound is about 406 VPH per lane. There are three peaks on both directions: at 8AM, 12PM, and at 5PM. The southbound traffic has a higher flow rate in the morning peak and has slight lower flow rate in the afternoon peak compared to the northbound traffic.

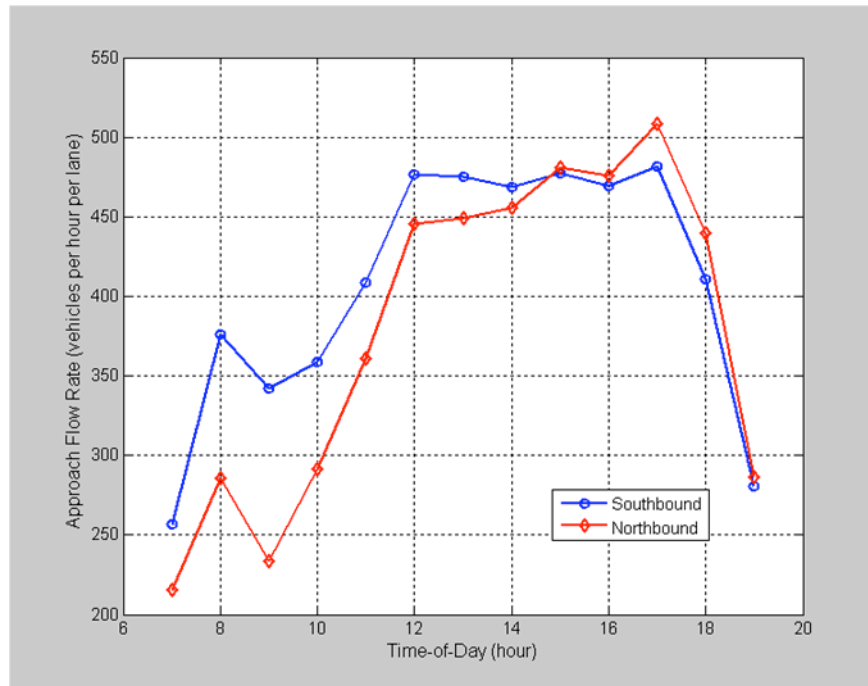


Figure 2-3 Approach Flow Rate as Function of Time-of-Day

In October 2004, a total of 403 northbound and 909 southbound RLR occurrences were detected. RLR frequency can be expressed as RLR occurrences per hour and per 1,000 entering vehicles. Table 2-2 summarizes the average RLR frequency for both directions. In average, there were about 5 RLR occurrences per hour (6 per 1,000 entering vehicles) on the southbound lanes and 2 RLR occurrences per hour and per 1,000 entering vehicles on the northbound lanes.

Table 2-2 Summary of RLR Frequency

Direction	Approach Flow Rate (VPH per Lane)	RLR Frequency	
		Occurrences per Hour	Occurrences per 1,000 Entering Vehicles
Southbound	406	4.72	6.28
Northbound	379	2.06	1.86

It is more interesting to see how RLR frequency varies by time-of-day when the approach flow rate changes. Figure 2-4 and Figure 2-5 plot RLR frequency in terms of occurrences per hour and occurrences per 1,000 entering vehicles, respectively as a function of time-of-day. The RLR frequency varies greatly by different time-of-day, especially in the early morning and late afternoon southbound direction.

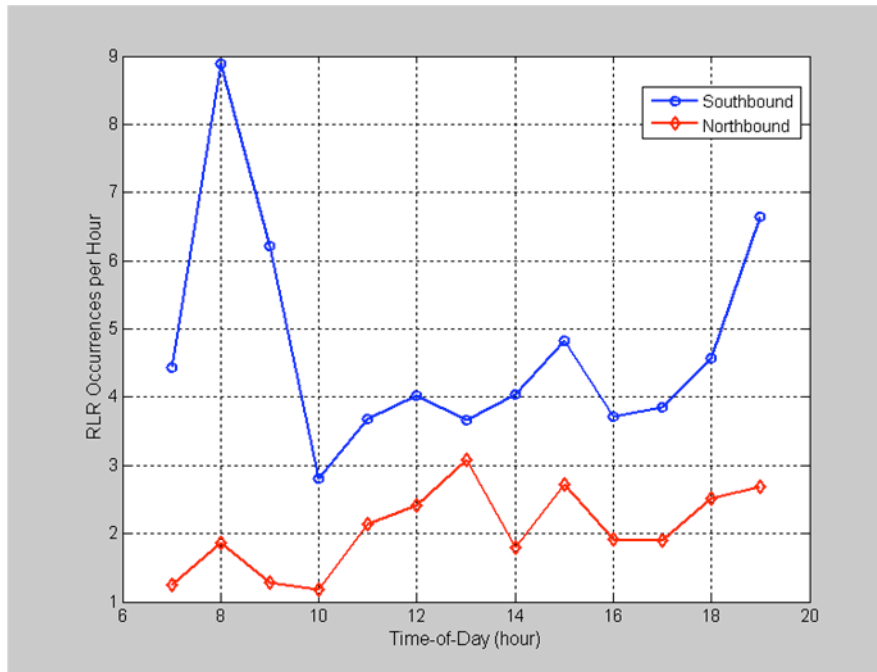


Figure 2-4 RLR Occurrences per Hour as Function of Time-of-Day

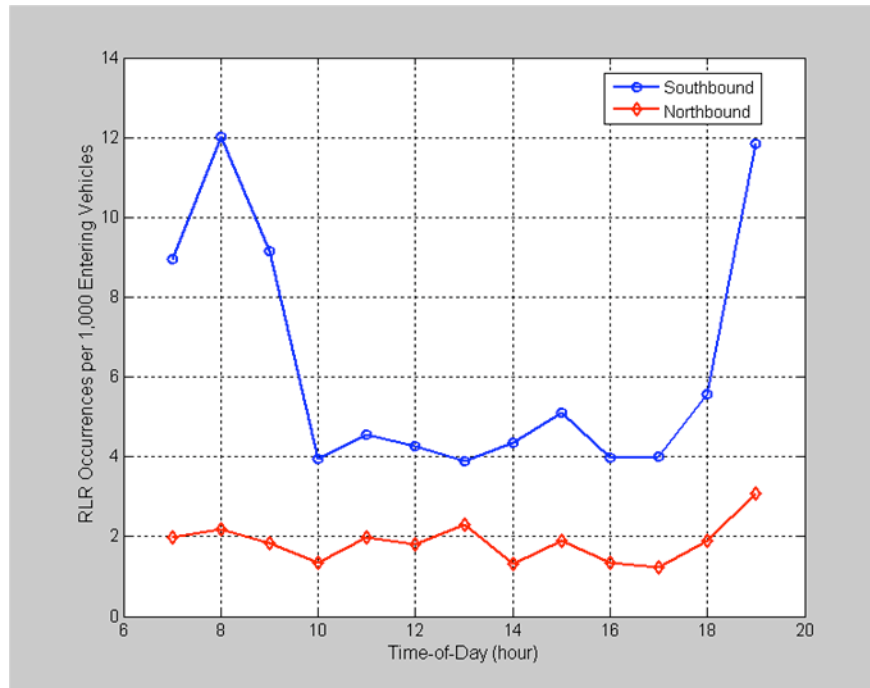


Figure 2-5 RLR Occurrences per 1,000 Entering Vehicles as Function of Time-of-Day

2.3.2 Red-Light-Running Frequency versus Approach Flow Rate

Several studies have reported that the RLR frequency is positively correlated with the approach flow rate (e.g., [2-1]). The correlation between RLR frequency and the approach rate was studied for the morning peak and afternoon peak on the southbound direction.

Figure 2-6 plots the correlation for the morning peak (7 AM – 10 AM). Each dot represents a sample of one-day’s observations. It clearly shows a strong positive correlation between RLR frequency and the approach flow rate (The straight line represents the linear regression line).

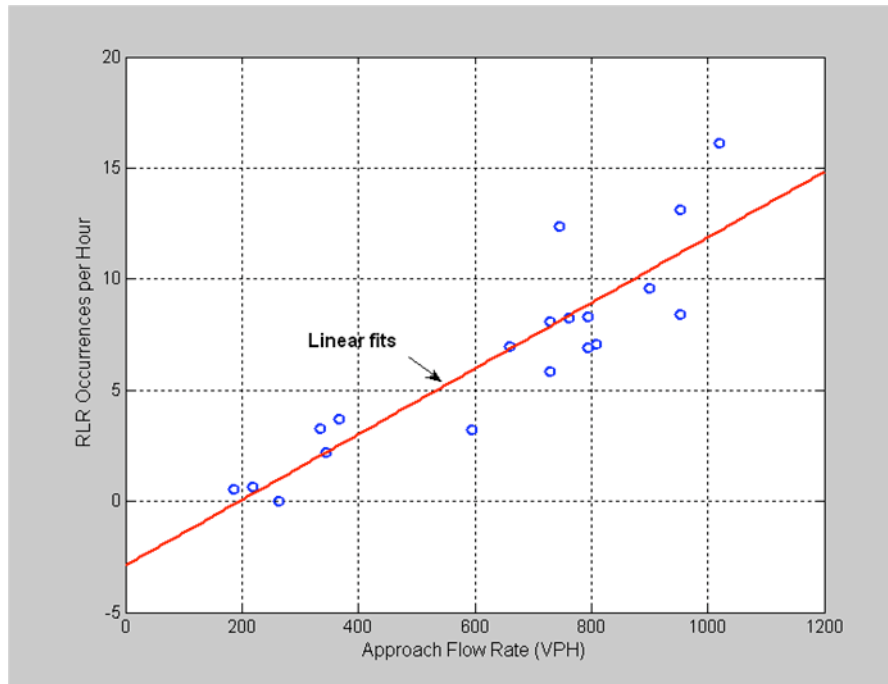


Figure 2-6 RLR Frequency vs. Approach Flow Rate (Southbound, 7 AM - 10 AM)

However, the trend is not that clear for the afternoon peak (4 PM – 8 PM), as shown in Figure 2-7. The difference in the correlations at different times-of-day (TOD) can be interpreted as a TOD factor, but it could also be influenced by factors that can not be identified by analyzing the aggregated traffic count information.

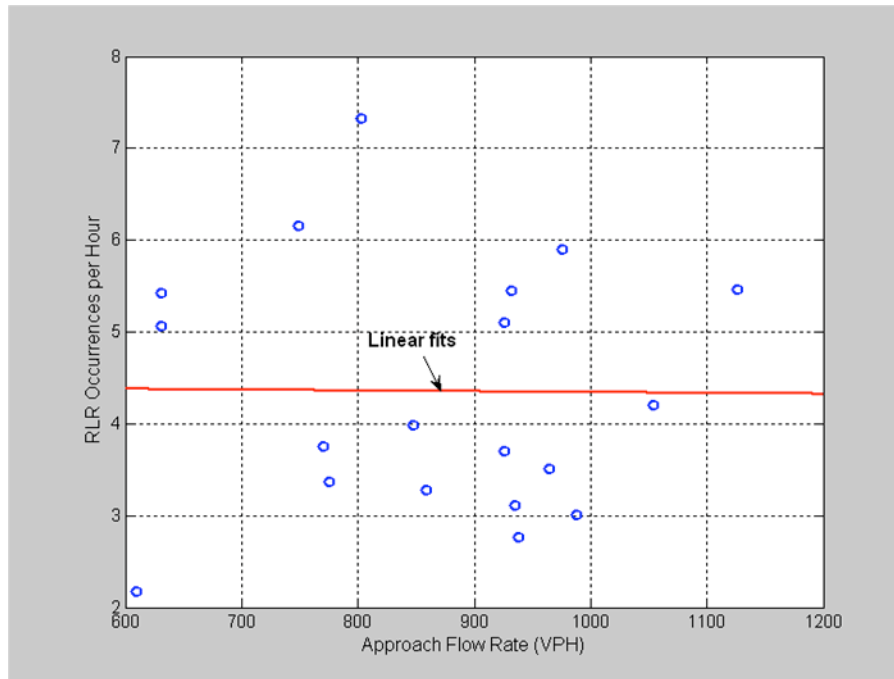


Figure 2-7 RLR Frequency vs. Approach Flow Rate (Southbound, 4 PM - 8 PM)

Because RLR occurs under specific momentary circumstances, it is essential to analyze the relevant factors within the smallest time frame for RLR. This time frame is the traffic signal cycle, starting from the onset of green phase to the end of red phase on the subject approach. Note that the definition of signal cycle here is different than the definition based on the local controller clock. On the latter definition, a green phase or a red phase on the subject approach could occupy two cycles, depending on the phase lead-lag condition.

A cycle-based data analysis is more desirable for studying RLR factors because each cycle includes one high risk period for RLR, i.e., the time interval during the signal phase transition. Furthermore, the potential contributing factors can be grouped into different time frames with

respect to the risk of RLR, i.e., green phase, yellow phase, and red phase, in order to isolate the relevant traffic operational factors.

2.4 Cycle-Based Data Analysis

2.4.1 Data Preparation and Processing

2.4.1.1 Definition of a Sample

In this study, the data set collected during every cycle represents a sample, and all variables are collected or averaged over a cycle. The cycle is defined as the time interval that starts at the onset of green phase and ends at the end of the red phase on the subject approach. The collected data consist of a total of 7,357 samples (signal cycles). To evaluate the impact of the different phases of the traffic signal, each sample has data for the green, yellow and red signal phases. The analysis is performed separately for each of the main traffic directions along the El Camino Real corridor.

2.4.1.2 Dependent Variable

The dependent variable used is an indicator variable. When the cycle has at least one RLR, the dependent variable takes the value of “1”, otherwise, the variable equals to “0”. The data for the dependent variable is collected from departure loops which are located at the stopline.

2.4.1.3 Independent Variables

The independent variables were selected based on findings of previous studies (e.g., [2-1]). In addition, the factor of the platoon being truncated at the onset of yellow on RLR is also

included. As drivers often travel in platoons through several interconnected signals, they expect that the green and yellow phase would be long enough for them to make it through the intersection and stay with the platoon. This optimistic expectation may result in RLR occurrences ([2-14]).

Table 2-3 Independent Variables Included in the Analysis

Variable name	Variable ID	Variable Description
Progression Ratio	G_COUNT_R	Total arrivals at the advance loop during the green phase, divided by the total arrivals at the advance loop during the cycle.
Green Flow	GRN_FLOW	The number of vehicle arrivals at the advance loops during the green phase.
Yellow Flow	YLW_FLOW	The number of vehicle arrivals at the advance loops during the yellow phase.
Red Flow	RED_FLOW	The number of vehicle arrivals at the advance loops during the red phase.
Termination of the Green	GRN_TER	Dummy variable indicating the type for terminating the green phase (gap-out, max-out, force-off).
Cross Traffic	CRS_GRN	The proportion of green time provided to the cross traffic
Time of Day	TOD	Dummy variable indicating time-of-day traffic control plan
Green Clustering	GRN_CLUS	Percentage of clustered vehicles of the green flow
Red Clustering	RED_CLUS	Percentage of clustered vehicles of the red flow
Clustered Vehicles Before Yellow Onset	N_BF_O_Y	The number of clustered vehicles ahead of the advance loops when a cluster is present, at the onset of the yellow phase
Clustered Vehicles After Yellow Onset	N_AF_O_Y	The number of clustered vehicles behind the advance loops when a cluster is present, at the onset of the yellow phase

Table 2-3 lists the independent variables included in this study as well as their descriptions.

The data for the independent variables were collected from the advance loops, located 60 meters upstream of the stopline, and reflect causal factors for the dependent variable.

The independent variables include the arrival flows during the different signal phases and other additional variables previously shown to impact RLR probability, such as progression

ratio, cross traffic, and the type of green phase termination. Since second-by-second data is used, estimations of the speed of any particular vehicle have significant estimation errors. As a result, speeds of individual vehicles are not included as part of this analysis.

Variables that represent the platoons in a traffic flow are also included. Vehicles following with headways of two seconds or less are defined as a cluster, and the proportion of clustered vehicles within the different signal phases is calculated. The percentage of clustered vehicles within the flow that arrived during the yellow phase was excluded from the analysis, since it is conceptually correlated with the yellow signal phase arrival flow. Furthermore, when a cluster is present at the onset of yellow phase, two variables are included: one to represent the number of vehicles within the cluster that have passed the advance loops (N_BF_O_Y) and the other to represent the number of vehicles within the cluster that are approaching the advance loops (N_AF_O_Y).

2.4.2 *Statistical Analysis Method*

Because of the binary nature of the dependent variable, a binary logistic regression model was used to estimate the parameters.

Let $\pi(x)$ be the probability for RLR (dependent variable). It could be calculated using:

$$\pi(x) = \frac{e^{g(x)}}{1 + e^{g(x)}} \quad \text{Eq. 2-2}$$

And the logit link function of the logistic regression which calculates the changes in the log-odds of the dependent variable (i.e., RLR probability) is given by:

$$g(x) = \ln\left(\frac{\pi(x)}{1 - \pi(x)}\right) = \beta_0 + \beta_1 \cdot X_1 + \beta_2 \cdot X_2 + \dots + \beta_I \cdot X_I \quad \text{Eq. 2-3}$$

where $X_i, i = 1, \dots, I$ are the independent variables and $\beta_i, i = 0, \dots, I$ are the estimated parameters. A positive value of β_i means that higher values of the corresponding variable increases RLR probability, while a negative β_i means that higher values of the variable decreases RLR probability.

To further interpret the logit of an independent variable, we convert it to its odds-ratio using $\exp(\beta_i)$ which tells us what happens to the odds-ratio of the dependent variable when X_i is increased by one unit while all other variables are kept as constants. We define $Odds_{new}$ as the changed odds-ratio in response to one unit increase of an independent variable. The new probability, $\pi_{new}(x)$, for the dependent variable in response to one unit increase of an independent variable is given by solving

$$Odds_{new} = \frac{\pi_{new}(x)}{1 - \pi_{new}(x)} \quad \text{Eq. 2-4}$$

We then obtain the change in probability as a result of one unit change in an independent variable. This way we can also estimate what impact the significant variables have on RLR probability and focus our study on the substantial ones.

2.4.3 Results of Regression Analysis

The logistics regression analysis is preformed using SPSS. The estimates obtained by the regression for southbound (phase 2) are shown in Table 2-4, and that for northbound (phase 6) are shown in Table 2-5.

Table 2-4 Parameter Estimates for the Selected Model (Southbound)

Variable name	B	S.E.	Wald	df	Sig.	Exp(B)
GCOUNT_R	-1.596	0.591	7.304	1	0.007	0.203
GRN_FLOW	1.676	0.371	20.403	1	0.000	5.342
YLW_FLOW	3.556	0.202	309.734	1	0.000	35.009
CRS_GRN	-1.180	0.655	3.250	1	0.071	0.307
N_BF_O_Y	0.024	0.011	4.831	1	0.028	1.024
Constant	-1.273	0.556	5.233	1	0.022	0.280

Table 2-5 Parameter Estimates for the Selected Model (Northbound)

Variable name	B	S.E.	Wald	df	Sig.	Exp(B)
GCOUNT_R	-1.199	0.406	8.708	1	0.003	0.301
GRN_FLOW	1.369	0.348	15.487	1	0.000	3.931
YLW_FLOW	1.642	0.134	149.528	1	0.000	5.167
RED_CLUS	0.508	0.209	5.898	1	0.015	1.662
N_BF_O_Y	0.028	0.012	5.228	1	0.022	1.028
Constant	-3.180	0.318	99.751	1	0.000	0.042

For both directions, Red Arrival Flow (RED_FLOW), Termination of Green (GRN_TER), Time-of-Day (TOD), Green Clustering (GRN_CLUS) and Clustered Vehicles after Yellow Onset (N_AF_O_Y_) are statistically insignificant at the 5% significant level.

Four variables were found to be statistically significant for both directions at the 5% significant level: Progression Ratio (G_COUNT_R), Green Arrival Flow (GRN_FLOW),

Yellow Arrival Flow (YLW_FOLW) and Clustered Vehicles before Yellow Onset

(N_BF_O_Y). The following observations are obtained:

- Higher progression ratios correspond to lower probability of RLR;
- Higher arrival flows during the green phase increase the probability of RLR;
- Higher arrival flows during the yellow phase increase the probability of RLR; and
- When a cluster is present in the advance loop area at onset of yellow phase, higher numbers of vehicles within the cluster that have passed advance loops increase the probability of RLR.

Cross-street Traffic (CRS_GRN) was found to be significant for the southbound but insignificant for the northbound. Red Clustering (RED_CLUS) was found to be insignificant for the southbound but significant for the northbound. This may be the factor of the T-shape intersection where the threat of right-angle collision is higher for southbound motorists than that for the northbound.

2.4.4 Impacts of Significant Variables

We assumed the variables found to be significant on both directions (phase two and phase six) represent characteristics which are less sensitive to individual intersection design and evaluated their impact on RLR probability. The changes of probability for RLR under different values of the variables are estimated using the odds ratio. To compare the impact among the significant variables, we calculated how the RLR probability changes when we change the variables from their average observed value to their maximum observed value. The

first benefit of this technique is that the result is unrelated to the units of each variable and RLR probability is evaluated based on a range that represents reasonable values to the extreme values of each variable. Furthermore, we are predicting a change in the probability within the observed range for each variable.

The change in probabilities for the progression ratio (G_COUNT_R) results in a 9.3% reduction in RLR probability for the southbound, and an 8.1% reduction for the northbound. The green arrival flow (GRN_FLOW) increases the RLR probability by 12% for the southbound and by 9.3% for the northbound. The yellow arrival flow (YEW_FLOW) is found to be the most substantial variable - it increases RLR probability by 32.7% for the southbound and by 11.7% for the northbound. The number of vehicles in a cluster that have passed the advance loops (N_BF_O_Y) has the least impact on RLR probability, which increases by less than 0.5% for both directions. These findings support our assumption that RLR is strongly correlated with the yellow phase and that increased flows during the yellow phase have a greater influence on RLR than the flows during the green phase.

2.4.5 Focusing on Yellow Arrival Flow

To further look into the area around the yellow phase we divided the time around the yellow interval to four sub-sections and collected the arrival flows for each of these sub-sections. The definitions of the included variables are listed in Table 2-6.

Table 2-6 Additional Variables Included in the Sub-Section Analysis

Variable name	Variable ID	Variable Description
Last two seconds of green	G_FLW_2	The number of vehicle arrivals at the advance loops during the last two seconds of the green phase
First two seconds of yellow	Y_FLW_02	The number of vehicle arrivals at the advance loops during the first two seconds of the yellow phase
Last two seconds of yellow	Y_FLW_24	The number of vehicle arrivals at the advance loops during the last two seconds of the yellow phase
First two seconds of red	R_FLW_02	The number of vehicle arrivals at the advance loops during the first two seconds of the red phase

Note that the data for these variables originates from the advance loops located 60 meters upstream from the stopline, or equivalently about four seconds of travel time prior to the stopline. A vehicle crossing the advance loop during the first two seconds of red would arrive to the stopline about six seconds into the red.

Another logistics regression analysis using SPSS was performed for each direction and the estimates obtained by the regression are shown in Table 2-7.

Table 2-7 Parameter Estimates for the Sub-Section Analysis

Variable name	B	S.E.	Wald	df	Sig.	Exp(B)
Northbound						
G_FLW_2	0.315	0.061	26.320	1	0.000	1.371
Y_FLW_02	0.538	0.053	102.995	1	0.000	1.713
Y_FLW_24	0.222	0.058	14.586	1	0.000	1.249
RED_CLUS	0.910	0.181	25.184	1	0.000	2.485
Constant	-3.814	0.118	1048.470	1	0.000	0.022
Southbound						
G_FLW_2	0.460	0.055	69.719	1	0.000	1.584
Y_FLW_02	1.135	0.062	331.455	1	0.000	3.112
Y_FLW_24	0.527	0.084	39.378	1	0.000	1.694
Constant	-2.529	0.048	2768.370	1	0.000	0.080

As can be seen, the arrival flows during the first two seconds of red for both directions were statistically insignificant and the coefficient estimated for Y_FLW_02 was higher than its adjacent sub-sections, i.e., 3.112 for the southbound and 1.713 for the northbound.

Furthermore, the coefficients estimated for the G_FLW_2 and Y_FLW_24 for each direction have similar values, i.e., 1.584 vs. 1.694 for the southbound and 1.371 vs. 1.249 for the northbound. The findings reveal that within the eight seconds around the yellow phase, the arrival flow during the first two seconds of the yellow phase has the most substantial impact on the probability of RLR, while the adjacent sub-sections are somewhat symmetric around it.

2.5 Discussion

We found that the increased arrival flows during the green phase have a strong correlation with increased RLR. Because the arrival flows were measured at the advance loops, the green arrival flow accounts for the majority of the total arrival traffic during the cycle. Therefore this finding validates previous findings about ADT. However, as a result of the detailed cycle-based analysis, the yellow arrival flow has shown a much larger influence on the probability of RLR and should receive greater attention.

The results from the sub-section analysis strengthen the notion that certain sections of the signal cycle are the source for RLR. Higher flow during the yellow sub-section indicates a higher chance that those vehicles are staying with a platoon (or cluster). As a consequence, truncating a platoon in the middle could increase the probability of RLR.

We acknowledge the fact that data used for analysis comes from only one intersection and there is a possibility that the results derived from the data might be relevant only for this specific site. However, the advantage of this analysis arises from the level of detail in the data and also from the large sample size. As RLR characteristics are site related, data from other study sites will be very useful to reveal if the above conclusion is universal. Nevertheless, the yellow arrival flow captures most of the motorists who need to make the stop or go decision during the signal phase transition.

It is reasonable to conclude that yellow arrival flow would be a fundamental influencing factor for RLR at intersections where the change interval is appropriately designed according to ITE's recommendation. Most importantly, the yellow arrival flow is a controllable parameter in traffic signal control operation. A mechanism that terminates the green phase based on the patterns of arrival flows can reduce the yellow arrivals and consequently reduce RLR probability and related collisions.

Taking account of yellow arrivals as a safety measure in the design of traffic signal timing plans is the most cost-effective way to further enhance intersection safety. The enhanced signal timing could reduce RLR occurrences and related collisions and subsequently the chances that motorists are being exposed to RLR hazards. The studies for developing this approach are presented in the following two chapters.

2.6 References

- [2-1] Mohamedshah, Y., Chen, L. and Council, F., Association of Selected Intersection Factors with Red Light Running Crashes. Conference Proceedings of the Institute of Transportation Engineers Annual Meeting. 2000.
- [2-2] Bonneson, J., Brewer, M., and Zimmerman, K., *Review and Evaluation of Factors that Affect the Frequency of Red-Light-Running*. Report No. FHWA/TX-02/4027-1. Washington, DC: Federal Highway Administration, 2001.
- [2-4] Kamyab, A., McDonald, T., Stribiak, J., Storm, B., and Anderson-Wilk, M., *Red Light Running in Iowa: The Scope, Impact, and Possible Implications*. Center for Transportation Research and Education. Ames, IA, December 2000.
- [2-6] Zhang, W.-B. et al., *Development of Adaptive Transit Signal Priority Systems*, University of California, Berkeley: Institute of Transportation Studies, California PATH Program, PATH Research Report UCB-ITS-PRR-2005, August 2005.
- [2-8] Manual on Uniform Traffic Control Devices for Streets and Highways. Federal Highway Administration. November 2004.
- [2-10] Retting, R. and Greene, M., Influence of Traffic Signal Timing on Red-Light Running and Potential Vehicle Conflict at Urban Intersections. *Transportation Research Record 1595*. 1997.
- [2-12] *Traffic Engineering Handbook*. Institute of Transportation Engineers. 1999.
- [2-14] Van der Horst, R. and Wilmink, A., Drivers' Decision-Making at Signalized Intersections: An Optimization of the Yellow Timing. *Traffic Engineering and Control*. December 1986.

3 DEVELOPMENT OF A SAFETY ENHANCED SIGNAL TIMING OPTIMIZATION MODEL

3.1 Motivation

Traffic signals are installed to guarantee the safe crossing of vehicles and pedestrians by providing the right-of-way to competing movements. With steadily increasing traffic demands, it was soon realized that, once traffic signals exist, they may increase or reduce the efficiency of the network operations depending on the signal control strategies chosen for specific intersections ([3-1]). A number of traffic signal control models and strategies have been developed to improve the efficiency of traffic control operations (e.g., [3-2], [3-3]).

Bad signal timing can cause RLR and result in collisions. A study by Shinar et al. ([3-4]) shows that signal synchronization not only improves traffic efficiency but also has safety benefits. The study showed that in synchronized corridors, the odds of running a red light are a 1/7 of the odds in non-synchronized corridors.

In coordinated systems, traffic signal operations are optimized using the control variables of green splits, offsets, cycle length, and phase sequence. These control variables are determined by solving an optimization problem to achieve one or more of the following objectives ([3-5]):

- Minimizing delay
- Minimizing number of stops
- Maximizing progression efficiency

- Minimizing queue length, and
- Maximizing system throughput.

Traditional traffic control models mainly focus on mathematically formulating the road network. Computational methods are used to solve for the optimal control variables while safety is usually used only as a constraint, i.e., the change interval and lost time in a cycle. However, there are unacceptably high frequency and severity of RLR related crashes at signalized intersections which may indicate that current design tools are insufficient. Hence the safety measure should be included as part of the optimization objective, along with the efficiency measures.

The cycle-based data analysis discussed in Chapter 2 suggests that the arrival flow during the yellow phase is the most significant influencing factor of RLR and consequently can be used as a safety measure. For given traffic conditions in steady-state, the control of yellow arrivals can be achieved through the control of offsets. These findings motivate the idea of “fine-tuning” the offsets to reduce the yellow arrival flow and consequently reduce RLR occurrences while maintaining the intersection efficiency.

3.2 Feasibility Study

The first step in the development of a safety enhanced signal timing optimization model is to study the dynamics among offsets, intersection delay, yellow arrival flow and vehicle platoons. To conduct this study, a software tool that simulates traffic flow in a network is required. TRANSIT-7F was chosen for its ability to model platoon dispersion, to provide

second-by-second flow profiles of vehicles on all links in the network and to evaluate the performance using a custom built measures of effectiveness (MOE) extractor. This study only uses the simulation functionality of TRANSYT-7F rather than the optimization function as the main focus is to investigate how intersection delay and yellow arrival flow vary with the shifting of offsets.

3.2.1 TRANSYT-7F Simulation Model

A TRANSYT-7F network was built to simulate the traffic control operation on a corridor along El Camino Real, California. This 0.7-mile-long highway corridor includes five signalized intersections: (1) Jordan, (2) Showers, (3) San Antonio, (4) Del Medio and (5) Los Altos, from southern to northern as shown in Figure 3-1. It covers a wide range of intersection types, from three-way to four-way and with moderate to heavy cross street traffic. For example, San Antonio is a critical intersection for this section and has coordination on both the main street and the cross street.

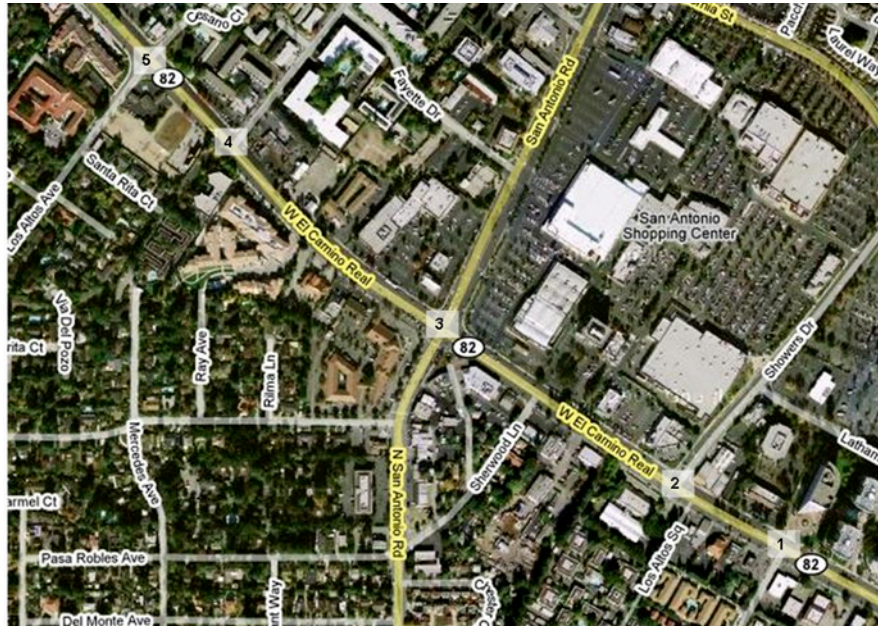


Figure 3-1 Aerial Photo of Study Site

To construct the model, traffic flows, intersection geometry, and the signal-timing tables in the field were collected for each link and intersection along the study section. The control variables in place match very well with the optimal solution from TRANSYT-7F.

Custom-designed software has also been developed to evaluate the outcome of changing the offsets. The software modifies the offsets, generates batch runs of the TRANSYT-7F model, and calculates the delay and yellow arrival flow for individual intersections. The outputs and diagrams are generated as a spread sheet.

3.2.2 Results for Isolated Intersections

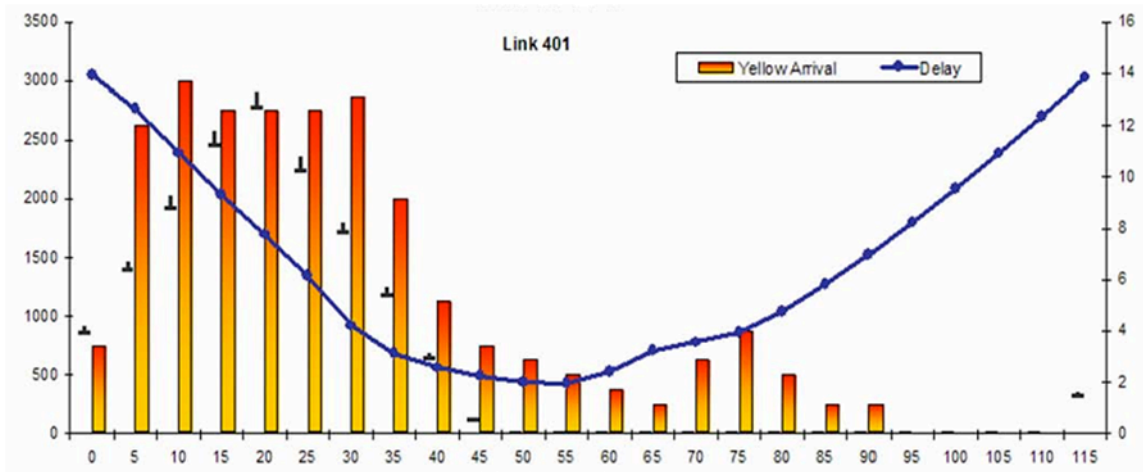
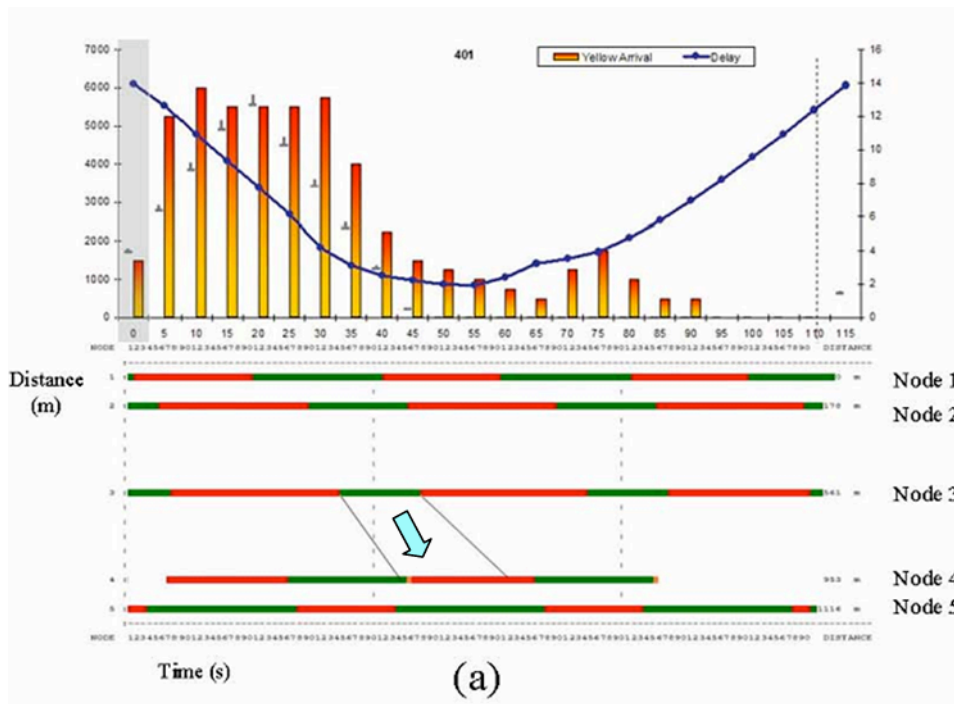


Figure 3-2 Delay and Yellow Arrivals as a Function of Offset

Figure 3-2 shows the delay and yellow arrival flow under different offsets for the northbound direction on node 4 (link 401). The horizontal axis represents the offsets in seconds for the subject current link. Each offset, in 5 second increments, represents the outcome of a separate TRANSYT-7F analysis and the values associated with it are on the vertical axis. The bars that correspond to the left-hand-side vertical axis represent the arrival flow during the yellow phase. The units are vehicles per hour (VPH) on the approach. The line corresponds to the right-hand-side vertical axis and represents the link delay. The units are vehicle-hours per hour. “⊥” signs in the figure are a coarse outline representing when the through platoon is truncated by the onset of the yellow phase. For each offset value, “⊥” signs to the right represent the through-flow vehicles that are truncated and “⊥” signs to the left represent the through-flow vehicles that are let through by the signal. For example, about half of the platoon is truncated with an offset of 20 seconds, while only about 20 percent are cut off with an offset of 40 seconds.

Figure 3-3 provides an intuitive explanation of the changes shown in Figure 3-2 and a demonstration of the potential benefits of shifting offsets. Each of the diagrams in Figure 3-3(a)-(c) has a time-space diagram corresponding to the offset marked by the vertical gray band. The time-space diagram shows the red phase and the green phase for all nodes. Two thin lines on each time-space diagram roughly represent the through-flow platoon traveling from node 3 to node 4. The line on the left represents the first vehicle in the platoon while the line on the right represents the last vehicle of the platoon. The sequence of the figures shows how changes in offsets affect the platoon coming from the node 3.



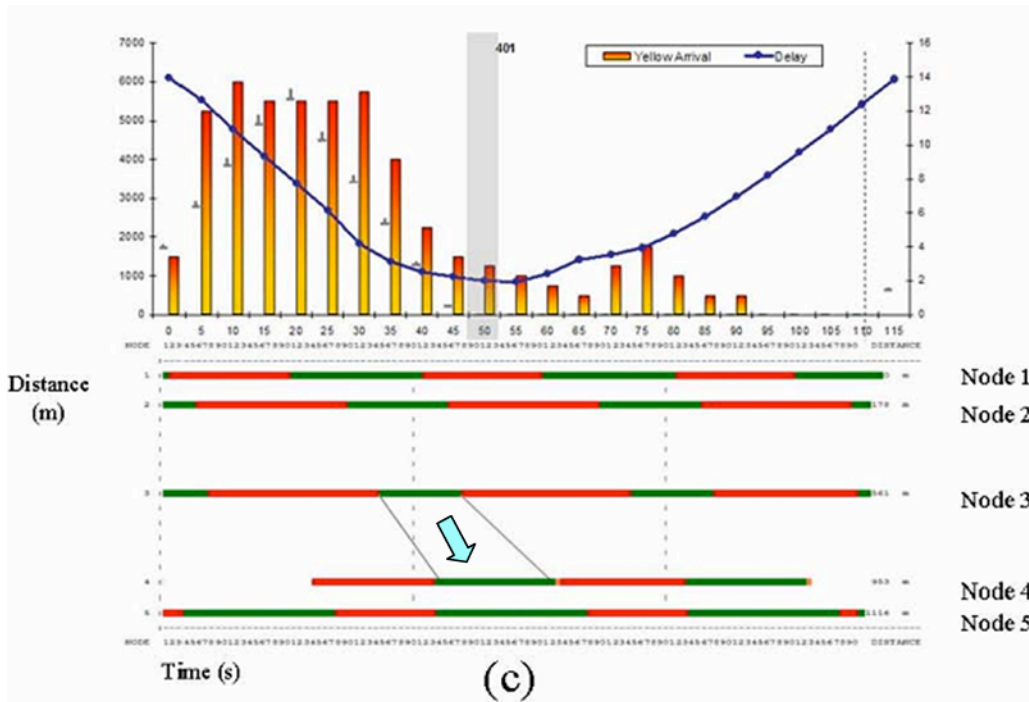
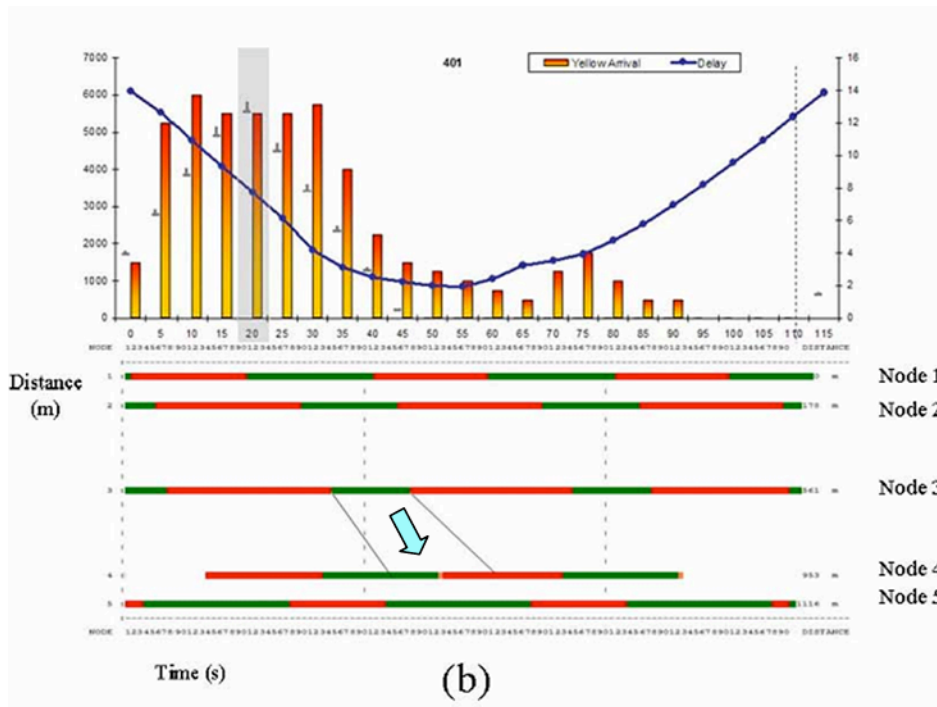
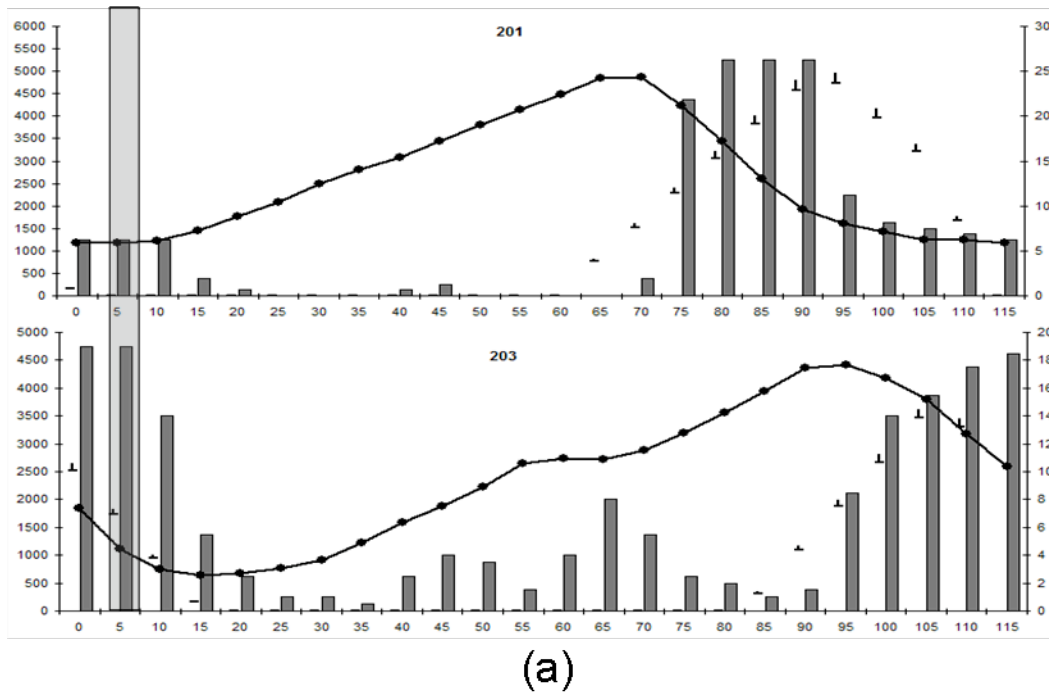
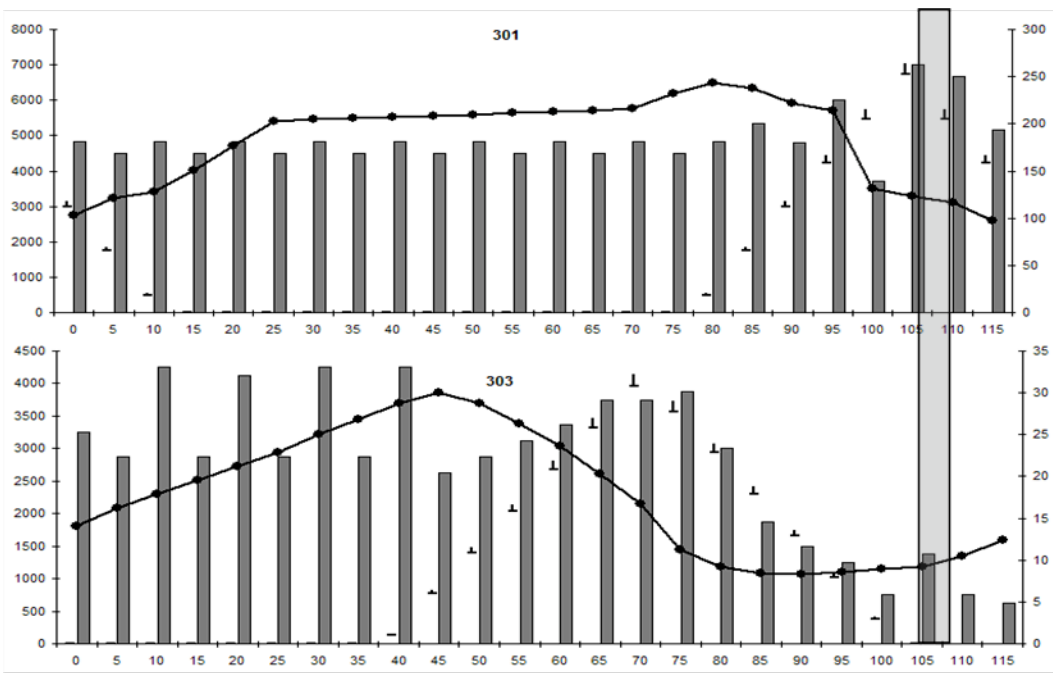


Figure 3-3 Delay and Yellow Arrivals with Time-Space Diagrams

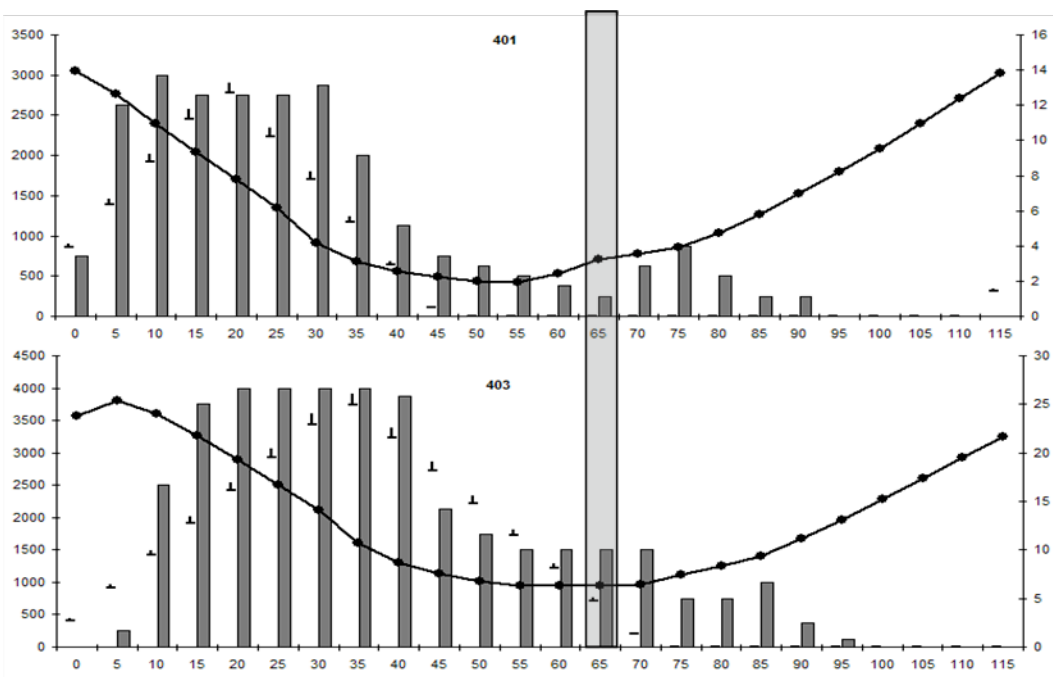
In Figure 3-3(a) with an offset of zero, only the very first vehicle in the platoon passes through the intersection, thus relatively low yellow flow is observed. Furthermore, since most of the platoon is stopped at this link, all vehicles have to wait for the next green phase. Hence the corresponding delay observed is high. In Figure 3-3(b), with an offset of 20 seconds, the truncation is around the middle of the platoon which is dense and corresponds to a high value of yellow flow. The delay is now reduced since fewer vehicles are required to wait at the intersection. In Figure 3-3(c), with an offset of 50 seconds, most of platoon passes through the intersection. Both the delay and yellow flow are low. Reviewing all intersections, it was observed that delays are usually minimal when only the very last part of the platoon is truncated and the corresponding yellow flow is also relatively low.

It is more complicated when both directions of an intersection are considered.





(b)



(c)

Figure 3-4 Delay and Yellow Arrival Diagram for Specific Links

Figure 3-4 displays diagrams for three intersections. It is clearly observed from Figure 3-4(a) that the delay and yellow flow on link 201 remain about the same if shifting the offset from the current value of 5 seconds to 10 seconds, while on the opposing link 203 both delay and yellow flow are reduced. Further shifting the offset to 15 seconds continues to reduce the yellow flow on link 203, while increases the delay on link 201. Thus the benefits of changing offset may need to be evaluated by applying weights on delay and yellow flow and an optimization mechanism that locates the optimal offset for an intersection could be established. Figure 3-4(b) and Figure 3-4(c) demonstrate different patterns due to the residual queues in node 3 and a different pattern of side street platoons on node 4, but the same concept still holds.

The main insight obtained from the results for isolated intersections is that there are situations when shifting the offsets can reduce yellow flow with little change in intersection delay. Furthermore, a framework has been established for optimizing the offset at an isolated intersection with respect to delay and yellow flow.

3.2.3 Results for the Corridor

For the corridor, analysis the same framework mentioned earlier was used but the calculation of delay and yellow flow is performed for the whole corridor in both directions. Figure 3-5 shows more diagrams for the five intersections. These diagrams are slightly different from the ones introduced earlier since the offsets start at the offsets currently used in the field instead of an offset of zero that was used before. Also note that each diagram shows the dynamics when only the offset for the study node changes while the offsets for the other nodes are fixed.

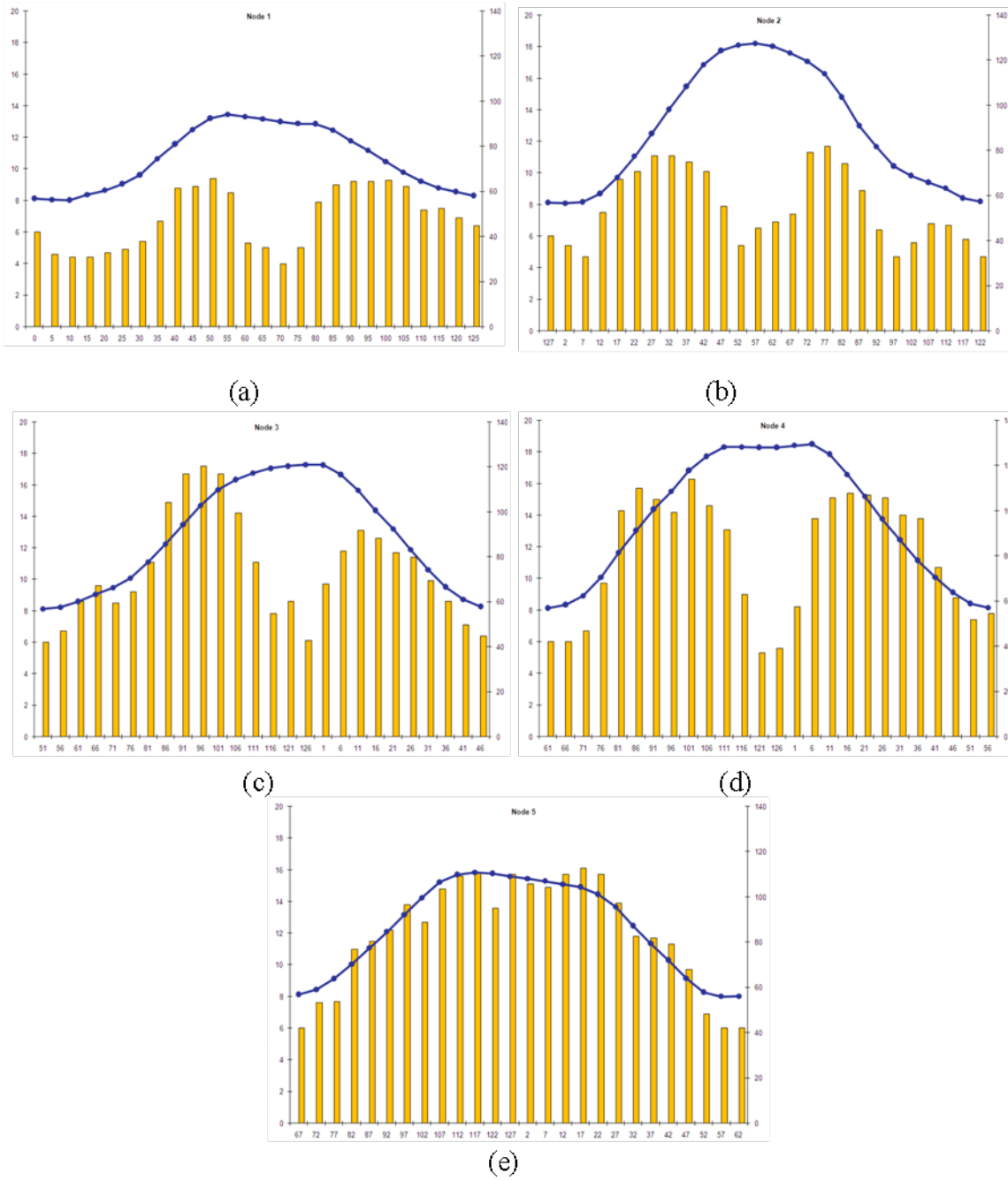


Figure 3-5 Delay and Yellow Arrival Diagrams for the Corridor

As shown in the diagrams, there are situations where a better offset exists for a single node with respect to the corridor. For example, at node 2 (Figure 3-5(b)) offsets of 122, 2 and 7 are better than the current offset of 127 due to the lower yellow arrival flow and similar total corridor delay. Similarly for node 1 (Figure 3-5(a)) shifting the offsets to values of 5 or 10 would be better than the current offset of zero.

Another observation from Figure 3-5 is that the current offsets (the left most offsets on each diagram) are reasonably close to, or sometimes even right at, the best offsets with respect to yellow arrival flow and total corridor delay. This is beneficial since the purpose of this analysis is not to redesign signal timing but rather to “fine-tune” the current offsets in a way that would provide safety benefits with a small compromise in traffic efficiency.

3.3 The Optimization Model

3.3.1 Formulating the Optimization Problem

Utilizing the findings from the previous sections, a basic optimization model was developed. The problem is formulated as a minimization issue with the objective function (or the cost function) defined as the weighted total corridor delay and yellow arrival flow, i.e.,

$$f = Total_Corridor_Delay + W \cdot (Corridor_Yellow_Arrival_Flow) \quad \text{Eq. 3-1}$$

The selection of weight, W , will be discussed later in this chapter.

For given control variables of green splits, cycle length and phase sequence, the cost, f , is a function of offsets. An iterative process was developed to seek the optimal offsets. The idea is

to find the “best” offset for a specific node while keeping offsets for other nodes as constants and then iteratively find the optimal offset for the rest of the nodes.

3.3.2 The Optimization Process

In order to have the iterative process finding the global optimum, two issues need to be addressed for the optimization algorithm. They are the selection of the starting point of the algorithm and the order of nodes to be optimized. An exhaustive analysis of all possible combinations of offsets was performed to identify the best starting point and the best order of the optimization iteration.

The best starting point is the optimal offsets for the corridor when only considering the conventional optimization criteria (e.g., total intersection delay). This finding matches with the observations described in the previous sections, i.e., the current offsets in the field are typically pretty close to the optimal offsets when taking the yellow flow into consideration.

Regarding the order of iteration, it was found that the best approach is to start from the most costly intersection in terms of the cost function and to continue iterating in decreasing costs. This makes sense because at each node the optimal offset is determined with respect to the total corridor delay and corridor yellow flow. More benefits can be gained from the node with higher cost. Therefore this iteration order can reduce the total number of iteration steps.

The flow chart of the developed optimization algorithm is shown in Figure 3-6. The process is terminated when the improvement rate is less than a predetermined threshold.

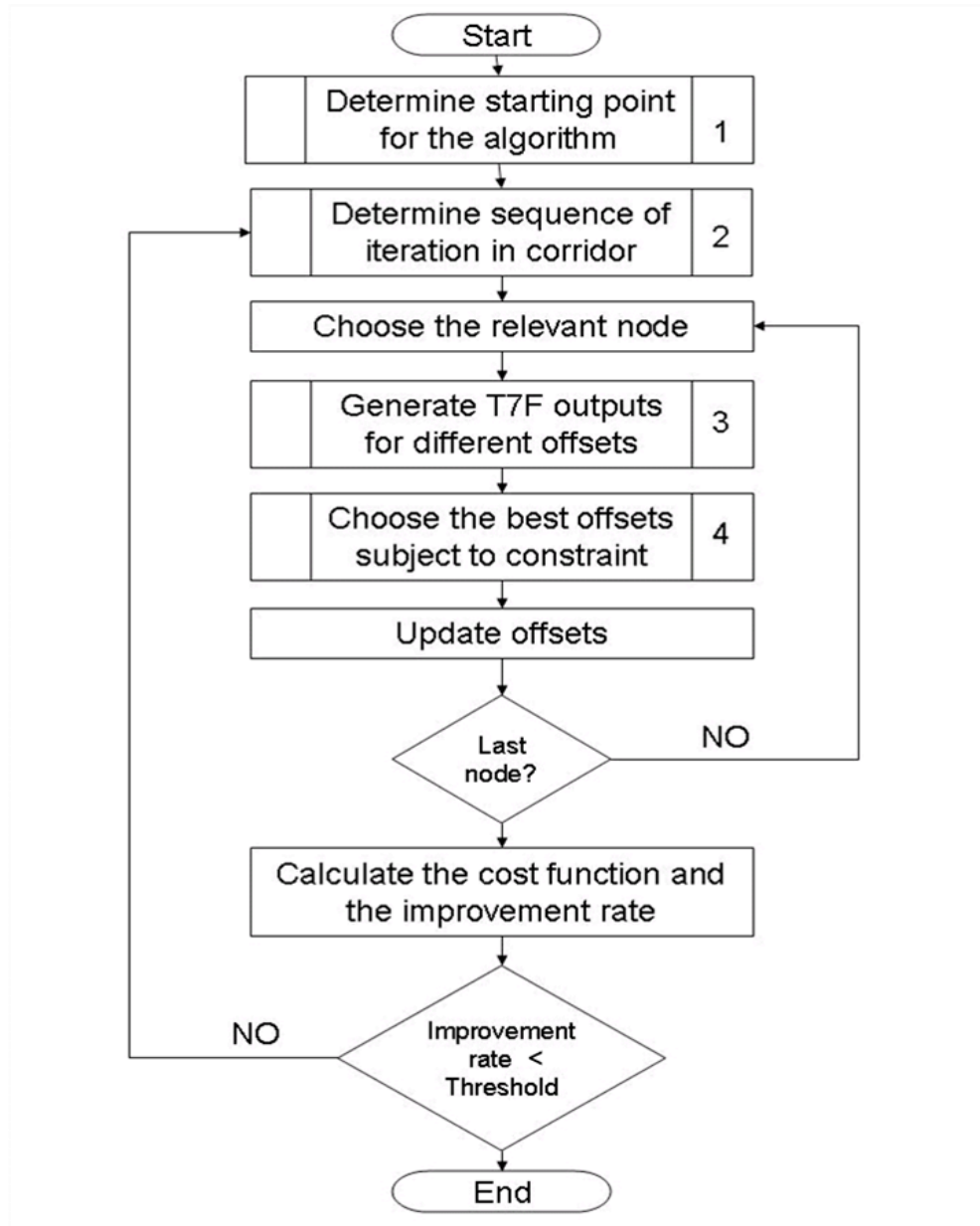


Figure 3-6 Flow Chart of the Optimization Algorithm

3.3.3 *Comparing to a Genetic Algorithm*

The developed offsets optimization algorithm was compared with the performance of a simple genetic algorithm (GA). However, since the GA implementation is not customized to consider and take advantage of the special features of the problem we are studying, it did not provide better optimization solutions and the exhaustive nature of the algorithm requires significant computation time (about 10 minutes for the 10 intersection case).

3.4 The Optimization Tool Package

This tool package consists of several components as shown in Figure 3-7. It is a combination of commercial software and custom-made software developed specifically for this study. The main component in the model is the Optimization Core which is based on the logic described in the previous section. On top of this core layer two custom-made programs were developed: the Batch Inserter that initiates a batch TRANSYT-7F process to generate the data requested by the Optimization Core and the MOE Extractor that extracts the newly generated data, reduces it, and feeds it back to the Optimization Core for the next optimization iteration. This model includes a user friendly interface.

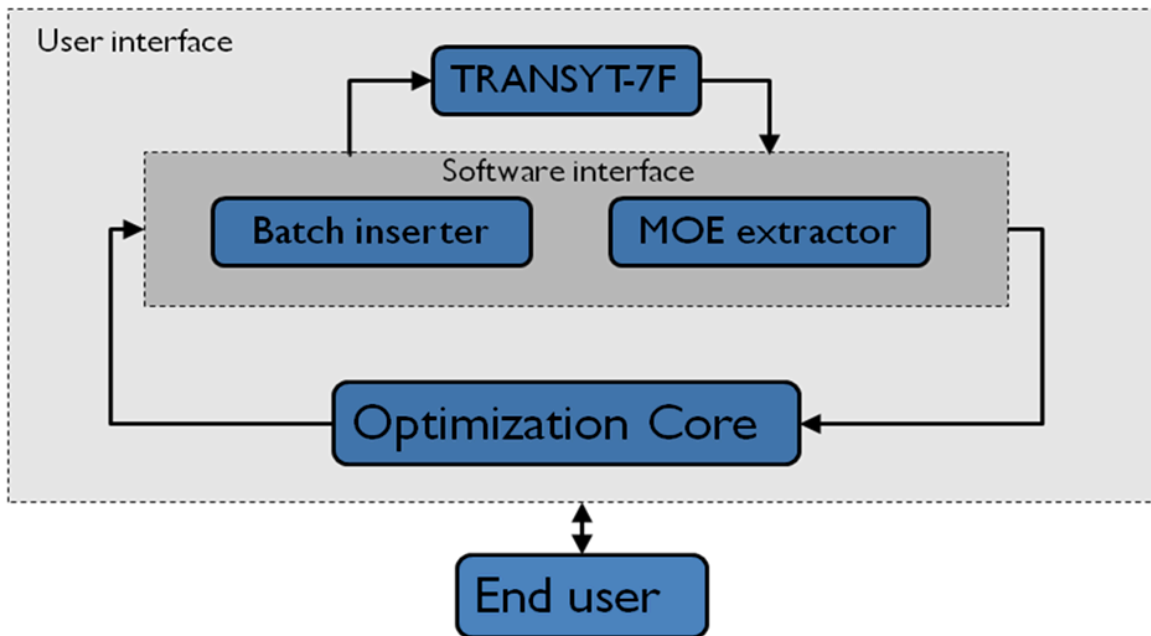


Figure 3-7 Architecture of the Optimization Tool

3.4.1 The Optimization Core

The Optimization Core uses the TRANSYT-7F model to determine the starting point and the order of iterations. It finds the optimal offset for the subject node and then provides a collection of offsets to the Batch Generator to generate data about the next node.

3.4.2 The TRANSYT-7F Model

To evaluate how various offsets would influence delay and yellow flow, a software tool is needed for an accurate representation of traffic flow. The TRANSYT-7F software package was select for this study, and the user needs to build a TRANSYT-7F model based on the traffic flows, signal timing and geometry of the relevant corridor.

It needs to be pointed out that other traffic flow simulation software can also be used as in the exploratory analysis. This is done only using the simulation capabilities of TRANSYT-7F. Additional development of the custom-made software is required to accommodate any changes in the input and output data files to the simulation software.

3.4.3 The Batch Inserter

The Batch Inserter is custom-made software written in C++. It is responsible for generating many TRANSYT-7F runs according to the requirements of the Optimization Core. It generates full TRANSYT-7F runs for each of the offsets combinations given by the Optimization Core for a predefined range and logs the data into data files.

3.4.4 The MOE Extractor

The MOE Extractor is also a custom-made program written in C++. It extracts the relevant data from the data file created by the Batch Inserter. Those data are then taken by the Optimal Core and used to evaluate the best offsets for this node. The MOE Extractor also extracts data not required by the Optimization Core but rather be used later by the user to evaluate the impact on other traffic related measures.

3.4.5 The User Interface

Since the optimization algorithm uses several types of software, a user-friendly interface was developed to execute this analysis. The interface was developed on MS Excel using Visual Basic for Application (VBA). The interface has a main screen, shown in Figure 3-9, where the

user sets the initial values for the analysis. The initial values include parameters of the corridor like the number of nodes, cycle length, initial offsets, and offset step size. The iteration-by-iteration results, including the number of the optimized node, are displayed in the table below the initial parameters.

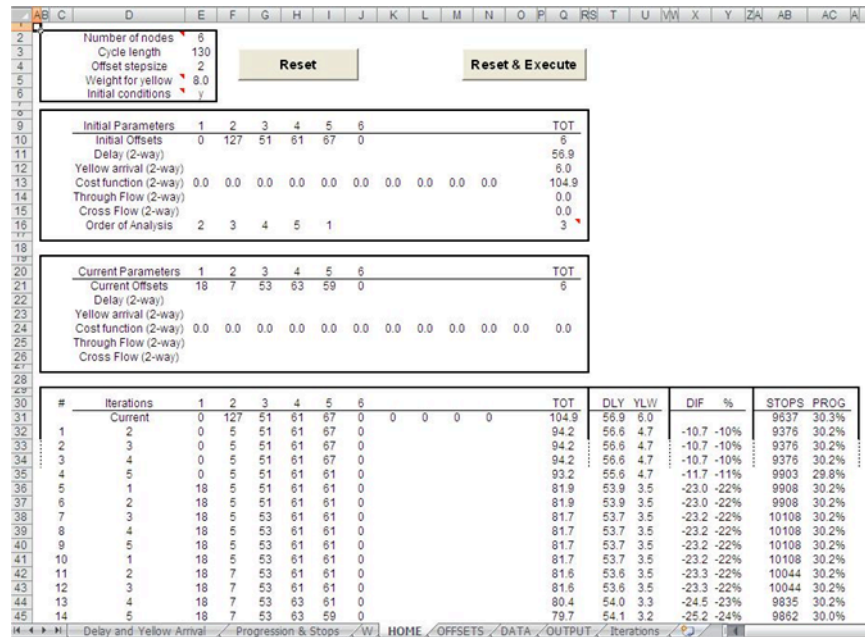


Figure 3-8 User Interface – Main Window

The results per iteration are also displayed in a graphic chart shown in Figure 3-9. The horizontal axis shows which node was optimized and the vertical axis represents the costs: delay (blue line), yellow arrival flow (yellow line) and the total weighted cost (green line). This diagram shows the user how the optimization improves from iteration to iteration.

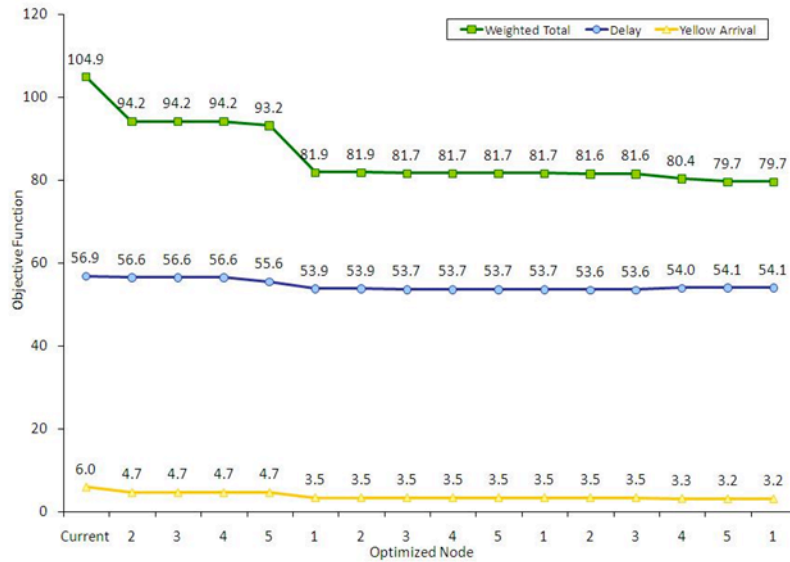


Figure 3-9 User Interface – Graphic Window

3.5 Considerations on the Weight

The objective function for the Optimization Core is a weighted combination of yellow arrival flow and delay, as shown in Eq. 3-1. A higher weight corresponds to an increased emphasis on safety, i.e., the yellow arrival flow or RLR frequency. Since there is a trade-off between intersection efficiency and safety, putting more emphasis on safety could have negative impact on the efficiency. The selection of the weight should address both efficiency and safety considerations.

The optimization tool has an evaluation function that helps a user to evaluate the impacts of weight on the efficiency and safety, and to select a desired weight based on an agency’s specific needs. The efficiency-related MOEs include delay, number of stops, and progression efficiency. The safety-related MOE is the yellow arrival flow.

Figure 3-10 shows how the values of yellow arrival flow and delay, achieved at the optimal offsets, would change corresponding to the changes in weight. The vertical axis is the delay and the horizontal axis is the yellow arrival flow. The black dot marked “current” corresponds to the values of yellow arrival flow and delay for the current offsets that are used in the field, and is used as the reference point for the selection of weight. The red line with arrow shows the trend of changes in yellow arrival flow and delay with increased weight.

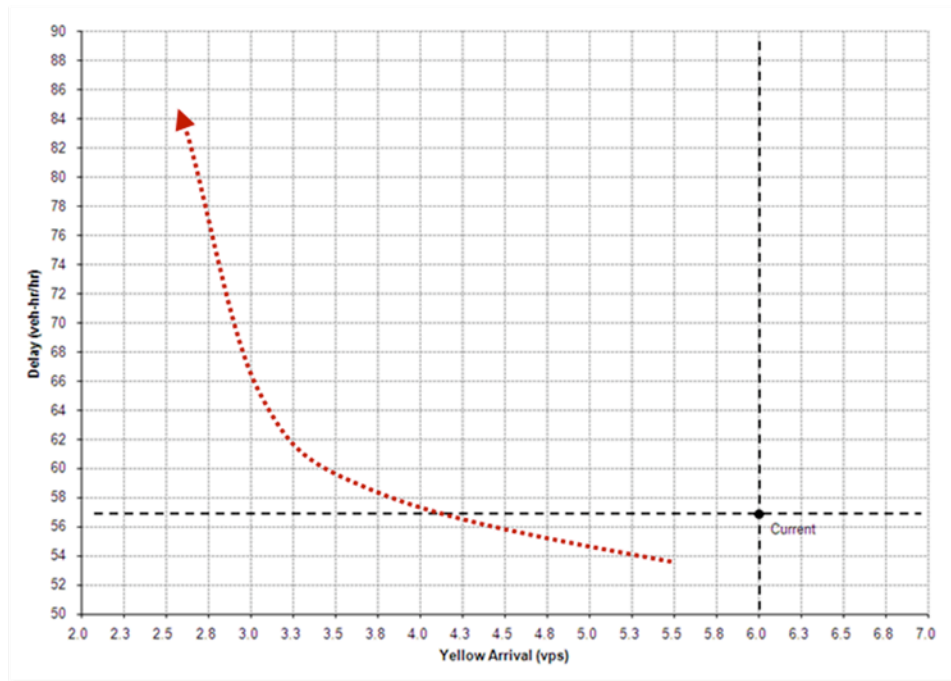


Figure 3-10 Yellow Arrival Flow and Delay as Functions of Weight

When the weight increases, the yellow arrival flow is reduced at the cost of increased delay. The figure also shows that there is a possibility to improve both delay and yellow arrival flow, where the red line is below the horizontal black dashed line. This is possible because the ‘current’ solution was obtained using a conventional optimization process which considers

objectives for maximizing the progression efficiency and minimizing the number of stops in addition to minimizing the delay.

Similar to Figure 3-10, Figure 3-11 shows the impacts of weight on traffic focusing on the MOEs on traffic progression and the number of stops. As can be seen, increasing weight corresponds to increased number of stops and decreased traffic progression. This makes sense as these two MOEs are not part of the Optimization Core process.

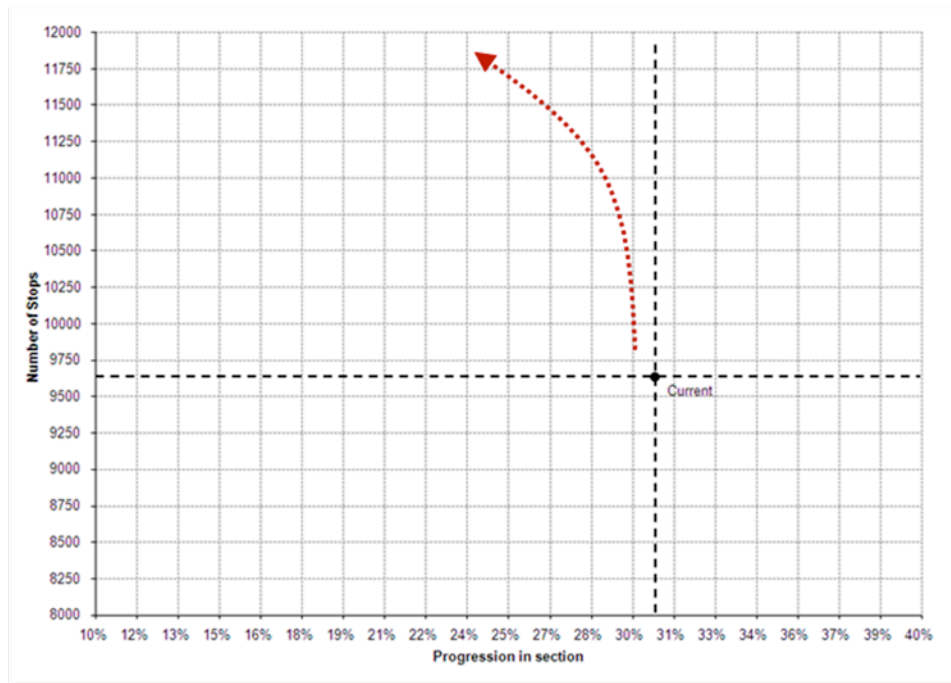


Figure 3-11 Progression and Number of Stops as Functions of Weight

For a selected range of weight, the optimization tool will generate the two graphic charts. This function enables the user to make an educated decision regarding the selection of weight and the corresponding optimal offsets.

3.6 References

- [3-1] Papageorgiou, M., Diakaki, C., Dinopoulou, V., Kotsialos, A., and Wang, Y., Review of Road Traffic Control Strategies (Contributed Paper). *Proceedings of IEEE*. Vol. 91, 2003.
- [3-2] Lo., H.K., A Novel Traffic Signal Control Formulation. *Transportation Research Part A: Policy and Practice*, Vol. 33, August 1999.
- [3-3] Skabardonis, A., Bertini, R. L., and Gallagher, B. R., Development and Application of Control Strategies for Signalized Intersections in Coordinated Systems. *Transportation Research Record 1634*. 1998.
- [3-4] Shinar, D., Bourla, M., and Kaufman, L. Synchronization of Traffic Signals as a Means of Reducing Red-Light Running. *Human Factors*, Vol. 46, 2004.
- [3-5] Chaudhary, N. A., Kovvali, V. G., and Mahabubul Alam, S. M., *Guidelines for Selecting Signal Timing Software*. Report No. FHWA/TX-03/0-4020P2. Washington, DC: Federal Highway Administration, 2002.

4 SIMULATION EVALUATION

4.1 Introduction

This chapter presents a simulation evaluation study of the performance of the proposed offset optimization algorithm in reducing the yellow arrival flow as well as the impacts on traffic.

The simulation evaluation study was performed using VISSIM, the leading microscopic simulation program for multi-modal traffic flow modeling. The benefits of conducting the simulation evaluation using VISSIM include:

- The microscopic simulation serves as testing tool for validating the performance of the algorithm prior to the field operational test.
- It is different from the macroscopic simulation tool, TRANSYT-7F which we used for the optimization algorithm. It can simulate coordinated semi-actuated traffic control while TRANSYT-7F simulates the fixed-timing traffic control, and VISSIM provides more realistic results.
- It can help to identify factors that are potentially missed in the development of the algorithm and further refine the algorithm.

4.2 The Study Arterial Corridor

The corridor for this evaluation study is based on the one that used for the development of the offsets optimization algorithm. We extend the network to the north for one more intersection, to Dinah's Court along El Camino Real, as these six intersections are coordinated for through progression. Figure 4-1 shows the map of the studied section.



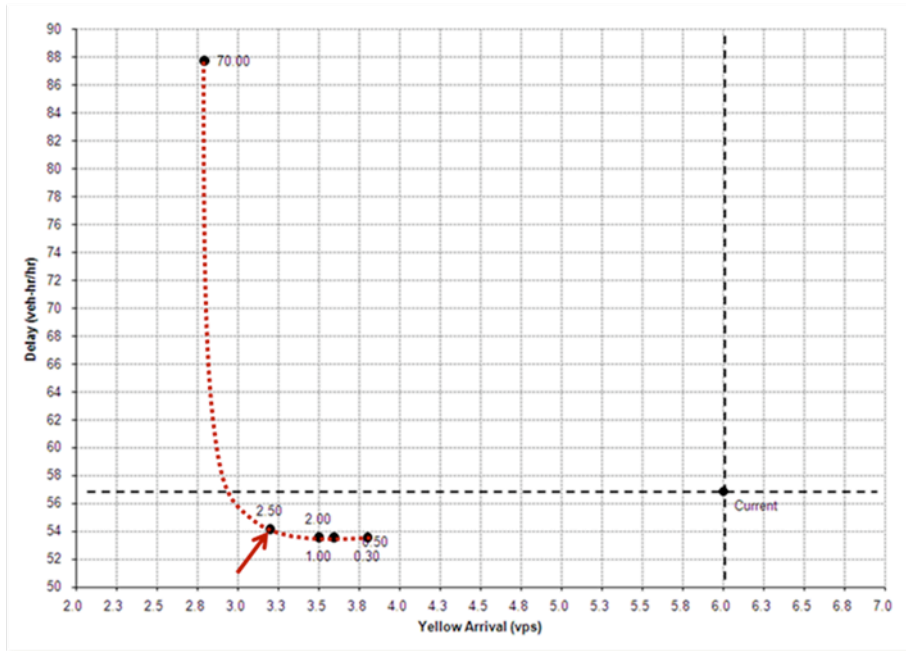
Figure 4-1 Aerial Photo of the Study Site

The analysis was preformed for the afternoon peak (3 PM – 7PM). The traffic control system in place provides coordinated and semi-actuated operation.

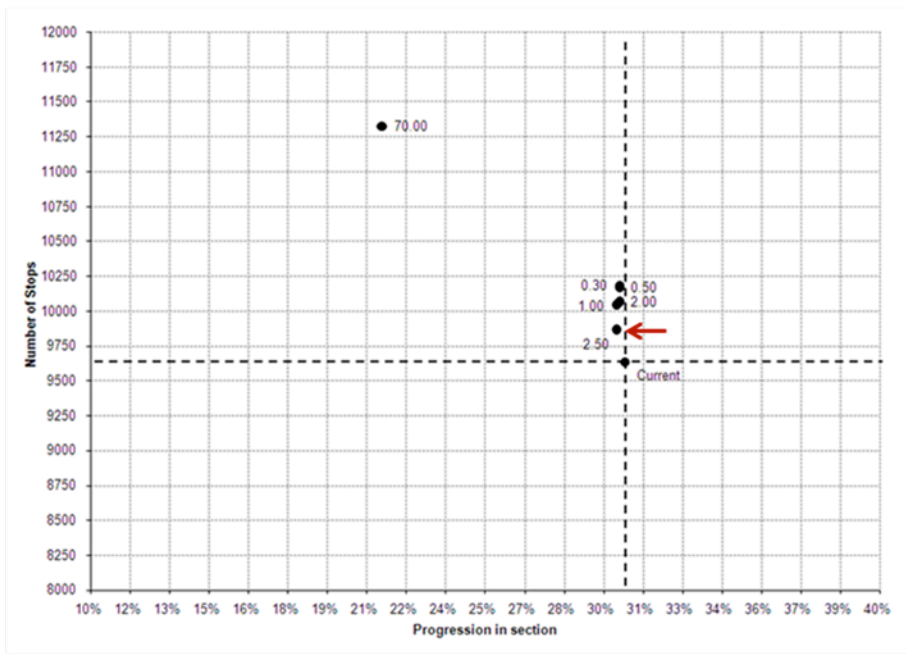
4.3 Optimization of Offsets

4.3.1 The Selection of Weight

Using the developed optimization tool, we conducted the sensitivity analysis for the weighting factor. The impacts on traffic and yellow arrival rates are shown in Figure 4-2. Again, the black dot marked “current” corresponds to the current offsets being used in the field. The weight for each point is marked and the red dotted line shows the approximate rate of trade-off. The unit for delay is vehicle hours per hour (veh-hr/hr) and the unit for yellow arrival is vehicles per second (vps).



(a)



(b)

Figure 4-2 MOEs as Functions of Weights

As shown in Figure 4-2(a), the yellow arrival flow for the current offsets is about 6 vehicles per second (vps) for all the six intersections of the corridor and the delay is about 57 vehicle-hours per hour. Both the delay and yellow arrival flow are reduced when the weight is below 2.5. However, if the weight is increased up to 70, the delay goes up significantly with no significant changes in the yellow arrival flow. In Figure 4-2(b), we can see that the number of stops is increased and the traffic progression is decreased at all points. The minimum negative impacts on traffic occur at weight of 2.5, where the changes in number of stops and traffic progression are both small. Therefore, the weight of 2.5 was selected.

4.3.2 The Optimization Process and Results

Figure 4-3 shows how the optimization progressed and how the yellow flow dropped from a value of 6.0 vps to a much lower value of 3.2 vps while the delay remains approximately at the same level, from 56.9 to 54.1 vehicle-hours per hour. The major benefits from the optimization were obtained rather quickly, after only one cycle of iterations.

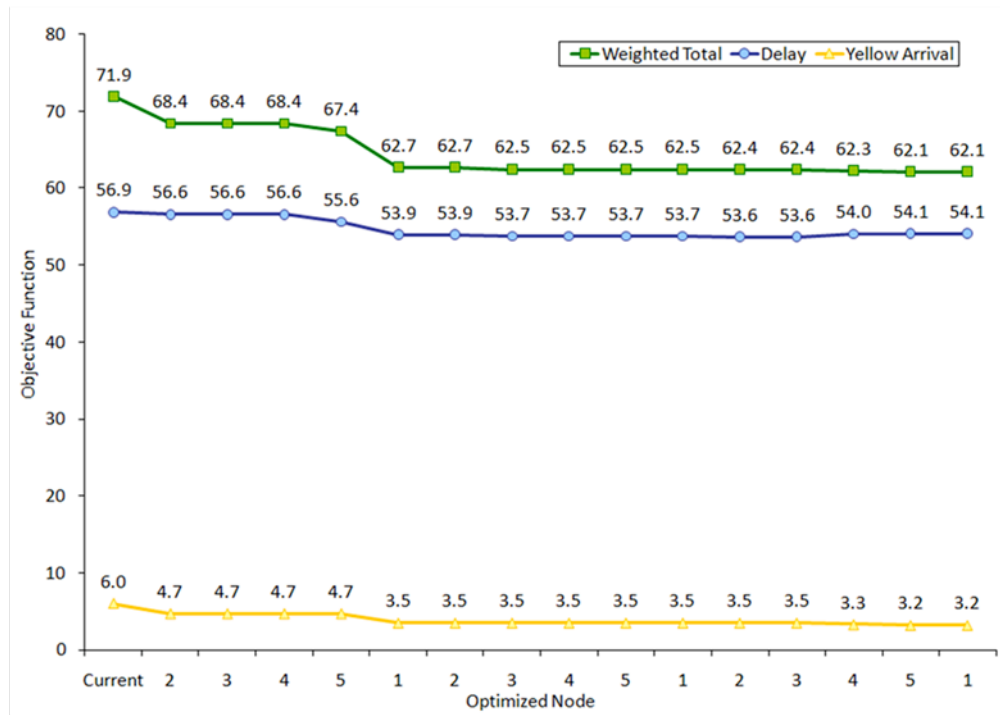


Figure 4-3 Optimization Results

Table 4-1 compares the current offsets with the optimal offsets. The changes in offsets are small on most of intersections, especially at the critical intersection for the studied corridor, the San Antonio Avenue.

Table 4-1 Comparison of Existing and Optimal Offsets

Cycle=130 sec	Dinahs	Los Altos	Del Medio	San Antonio	Showers	Jordan
Current Offsets	0	67	61	51	127	0
Optimal Offsets	0	59	63	53	7	18
Offsets Change	-	-8	+2	+2	+10	+18

Table 4-2 summarizes the changes in MOEs (delay, number of stops, traffic progression, and yellow arrival flow).

Table 4-2 Comparison of MOEs

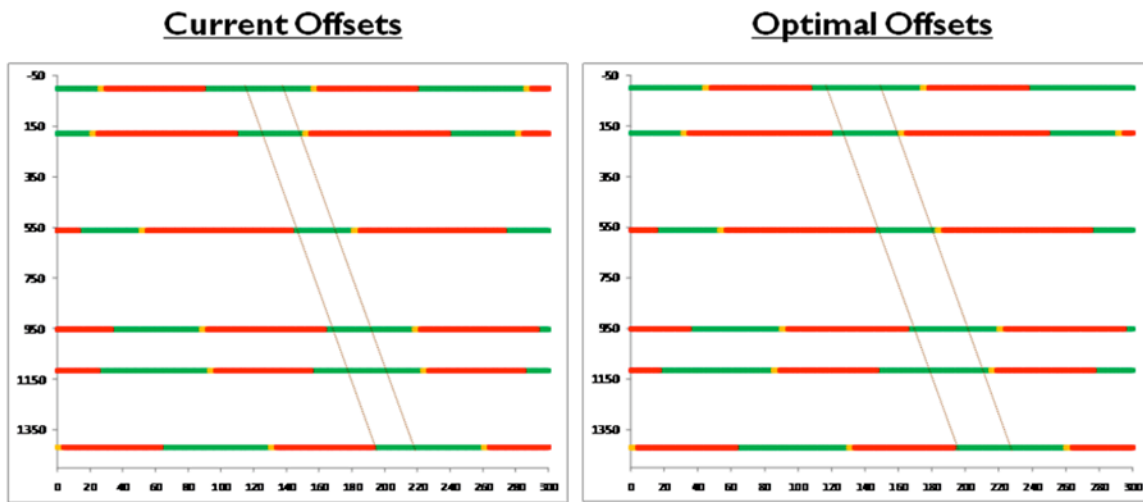
	Delay (veh-hr/hr)	Delay (sec/veh)	Yellow Flow (vps)	Stops (veh/hr)	PROS (%)
Current	57.0	13.3	5.97	9,637	30.3%
Optimum	54.2	12.7	3.19	9,862	30.0%
% Change	-4.9%	-4.6%	-46.5%	+2.34%	-0.3%

The results show that the yellow arrival flow was significantly reduced by 46.5 percent, the average per vehicle delay was reduced 0.6 seconds (4.6 percent). The degradation of traffic-related MOEs was minor, i.e., the number of stops increased by 2.3 percent, and the progression dropped by 0.3 percent.

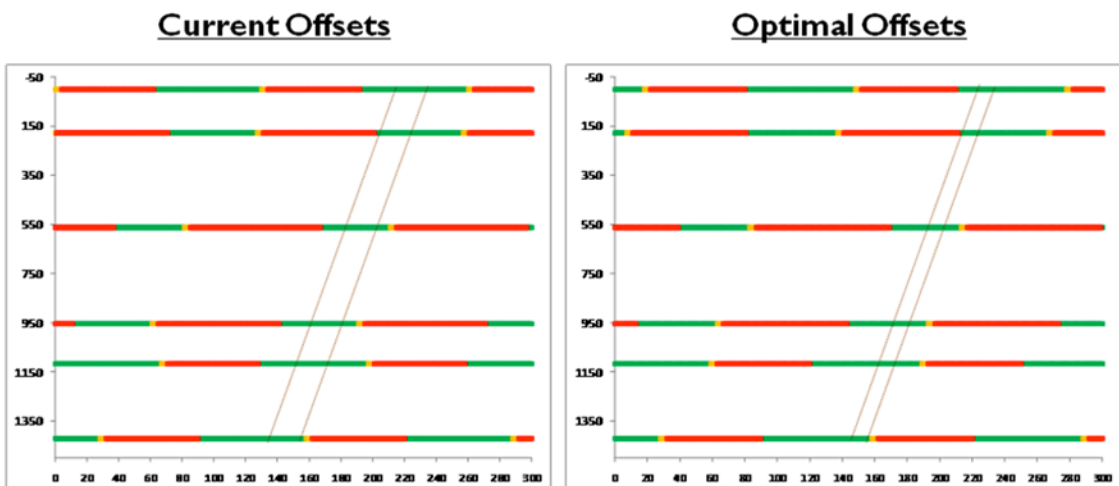
According to the statistical analysis presented in Chapter 2 of this report, the significant reduction in yellow arrival flow should have a corresponding impact on reducing RLR occurrences and therefore potentially improving the intersection safety. It is important to point out that this improvement in safety is obtained with negligible impacts on the traffic control.

4.3.3 Comparison of Green Band

Green band is another traffic-related MOE and has been applied in the design of coordinated signal timing (e.g., [4-1]). If a vehicle stays within the green band as it goes through signalized intersections, it will continue unopposed by a red light. Figure 4-4 shows the comparison of traffic green bands for southbound and northbound. The green band for the northbound direction becomes larger with the optimal offsets, and consequently the green band for the southbound direction is smaller.



(a) Northbound



(b) Southbound

Figure 4-4 Comparison of Green Band

4.3.4 Analysis for Individual Intersections

The objective of the offsets optimization algorithm developed in this study is to minimize the weighted sum of delay and yellow arrival flow for the 6-intersection arterial. However, it is also essential to observe the impact on each individual intersection.

4.3.4.1 Comparison of Yellow Arrival Flows at Individual Intersections

Figure 4-5 shows the comparison of yellow arrival flow for each individual intersection.

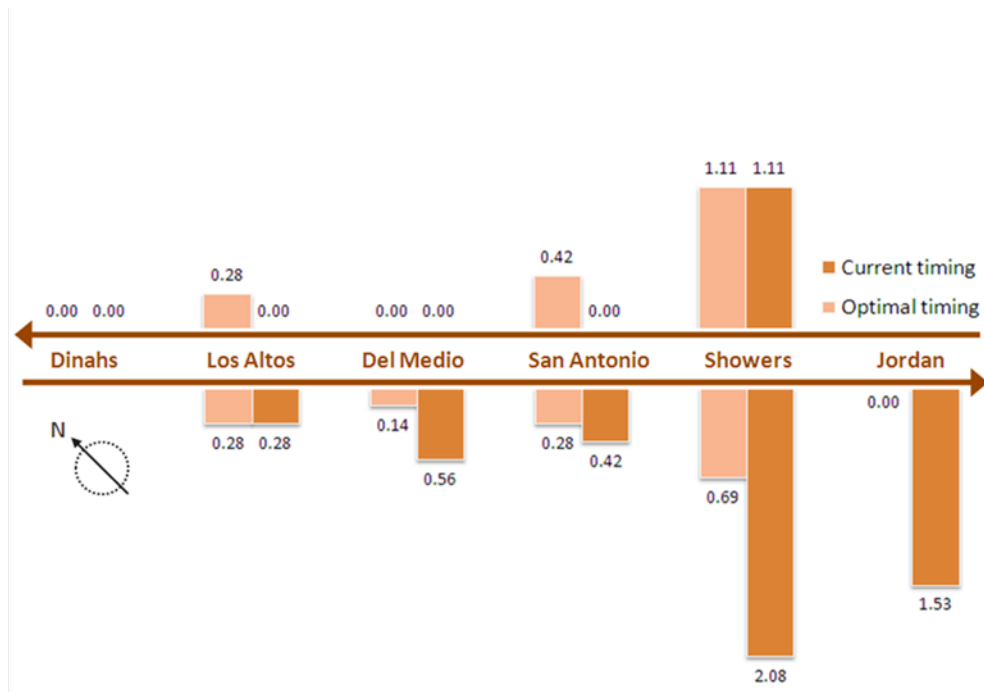


Figure 4-5 Comparison of Yellow Arrival Flow for Individual Intersections

With the original offsets, the southbound direction has much higher yellow arrival flow than the northbound direction. With the optimal offsets, the following observations are made from Figure 4-5:

- It reduced the overall yellow arrival flow on the corridor;

- It reduced the maximum yellow arrival flow; and
- It reduced the variance of yellow arrival flow among intersections.

4.3.4.2 Comparison of Delays at Individual Intersections

Figure 4-6 shows the comparison of delay for each individual intersection. The distributions of delay among intersections are very similar to the current offsets and the optimal offsets.

Overall the delays were reduced by 3 percent on the northbound direction and by 6.9 percent on the southbound direction. The changes are small and within the range of statistical error.

The important observation from Figure 4-6 is that the optimization of offsets maintains the level of delay at individual intersections.

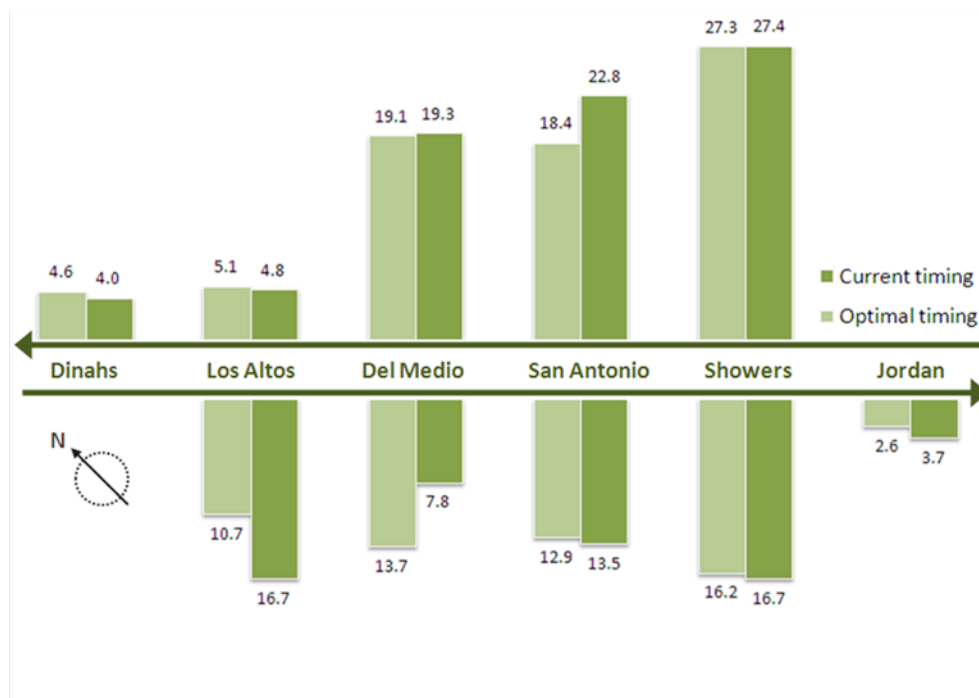


Figure 4-6 Comparison of Delay for Individual Intersections

4.4 Simulation Validation using VISSIM

4.4.1 The Simulation Model

As a microscopic modeling tool, VISSIM specializes in accurate network representation, detailed modeling of traffic dynamics, and realistic MOEs collection in the simulated network. Thus, it can be a good evaluation tool for verification and refinement of the offsets optimization model before the field operational test.

4.4.2 VISSIM Network Building

A VISSIM network was built to represent the traffic control operation on the study corridor, including the edits of road geometry, signal timings and traffic demands.

In VISSIM, the road geometry edit is done in a way that directly maps to the real world. With link and connector as two basic elements, VISSIM can represent the road geometry with great accuracy and flexibility. Figure 4-7 shows an intersection layout in VISSIM environment with the street level background.

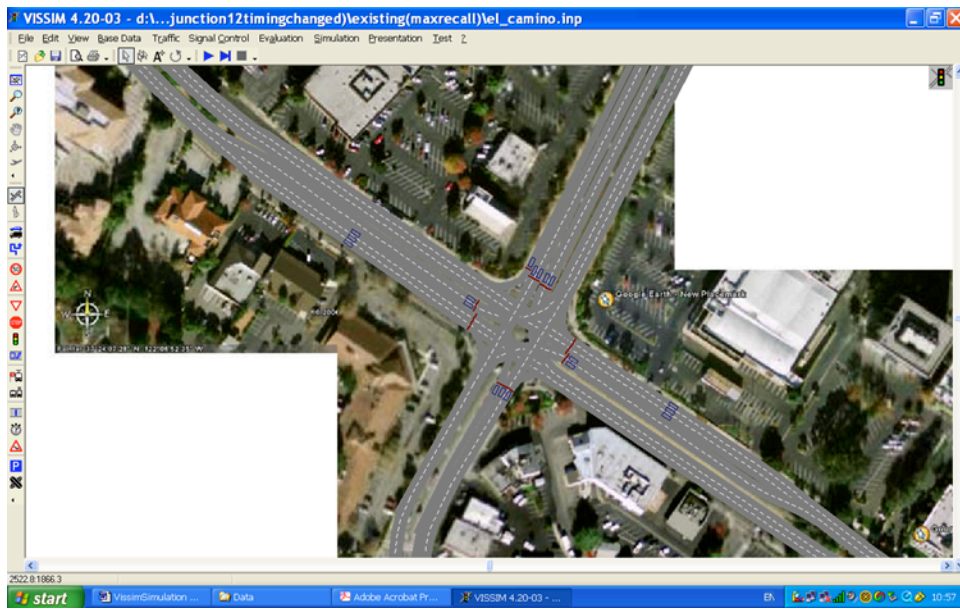


Figure 4-7 An Intersection Layout in VISSIM with Real-World Background

Figure 4-8 shows a bird's-eye view of the study arterial along El Camino Real in Santa Clara County, CA.

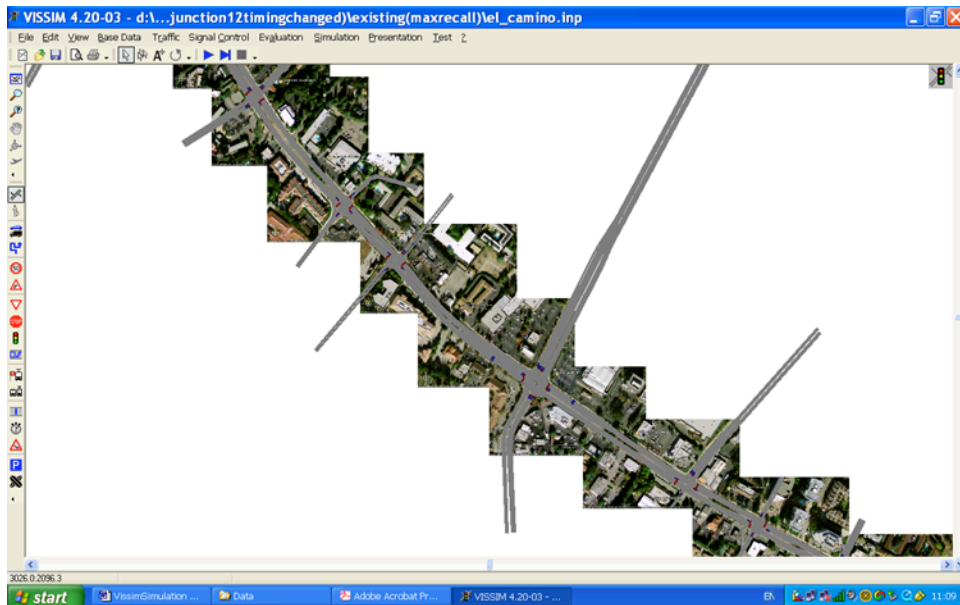


Figure 4-8 A Bird's-Eye View of the Study Corridor Stretch in VISSIM

VISSIM has a NEMA standard signal controller emulator module, which can simulate fully actuated signal control as well as coordinated and semi-actuated signal control. The existing controllers in the El Camino Real corridor are Model 170E controllers together with Caltrans C-8 Traffic Control software. There are some differences in parameter definitions between the C-8 software and the NEMA software. The major difference is on the definition of local zero point or the yield point. In C-8 software, the cycle zero point is defined as the green end time of the coordination phase, while in the NEMA software the local zero point is the green start time of the coordination phase in the first ring. A program was developed to transform the timing parameters from C-8 software to VISSIM NEMA emulator.

4.4.3 Origin-Destination (OD) Matrix

Different than TRANSYT-7F model which uses link flow to generate the flow on the corridor, the VISSIM model uses OD matrix. The link flows collected from the field was transformed to OD matrix using a simple OD program for the VISSIM model.

4.4.4 MOE Collection

The measures of effectiveness (MOEs) collected include the delay, number of stops and yellow arrival flow at individual intersections. The standard VISSIM module is used to collect the delay and the number of stops (see Figure 4-10). However, the yellow arrival count is not available in the standard module. The collection of yellow arrivals is achieved through VISSIM COM-programming.



Figure 4-9 Collection of Measures of Effectiveness in VISSIM

4.4.5 *Simulation Results*

As the OD matrix used by the VISSIM model was transformed from the link flow used by the TRANSYT-7F model, it is essential to compare the link flow generated by the VISSIM model with that used by the TRANSYT-7F model to validate the transform calculation.

Figure 4-10 provides such a comparison. As can be seen, although the absolute values of flow may be slightly different but the overall pattern is almost the same for both simulation models.

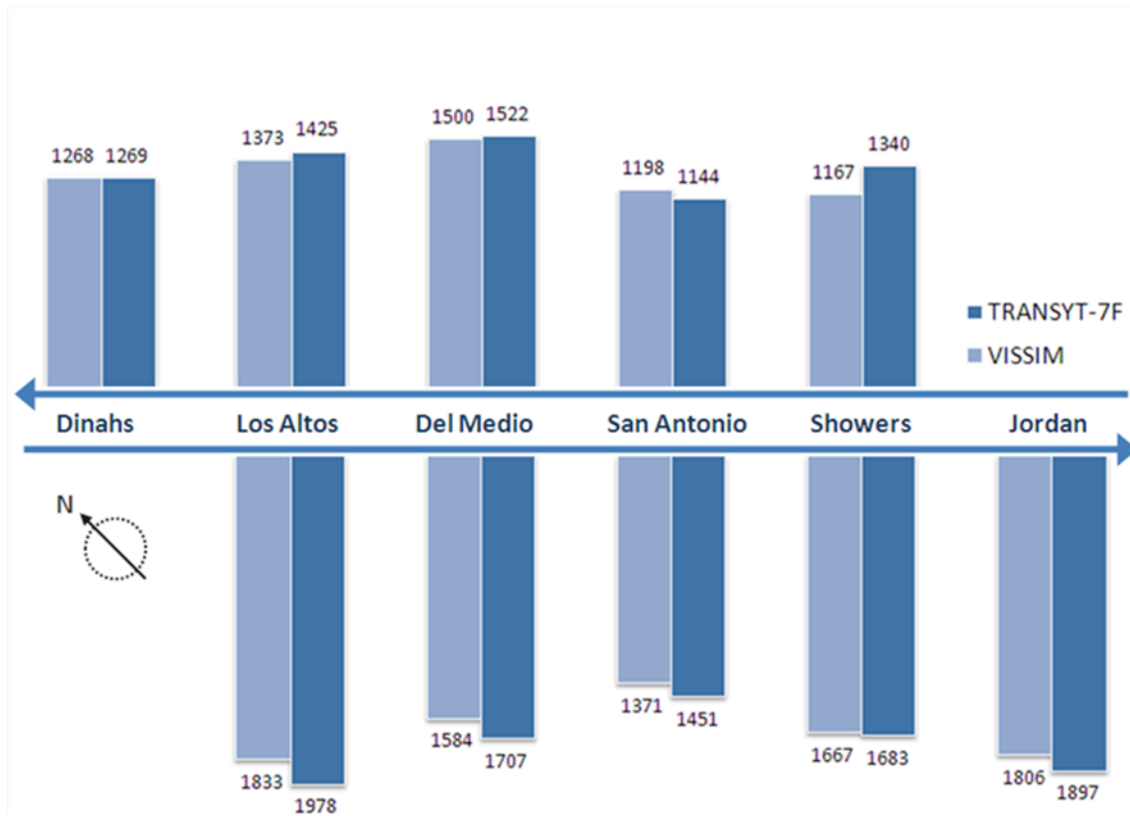


Figure 4-10 Flow per Link for the Current Offsets

Figure 4-11 compares the delay per link for the two simulation models. Again, the absolute values of delay are different but the distribution and the pattern of delay amongst the intersections are quite similar.

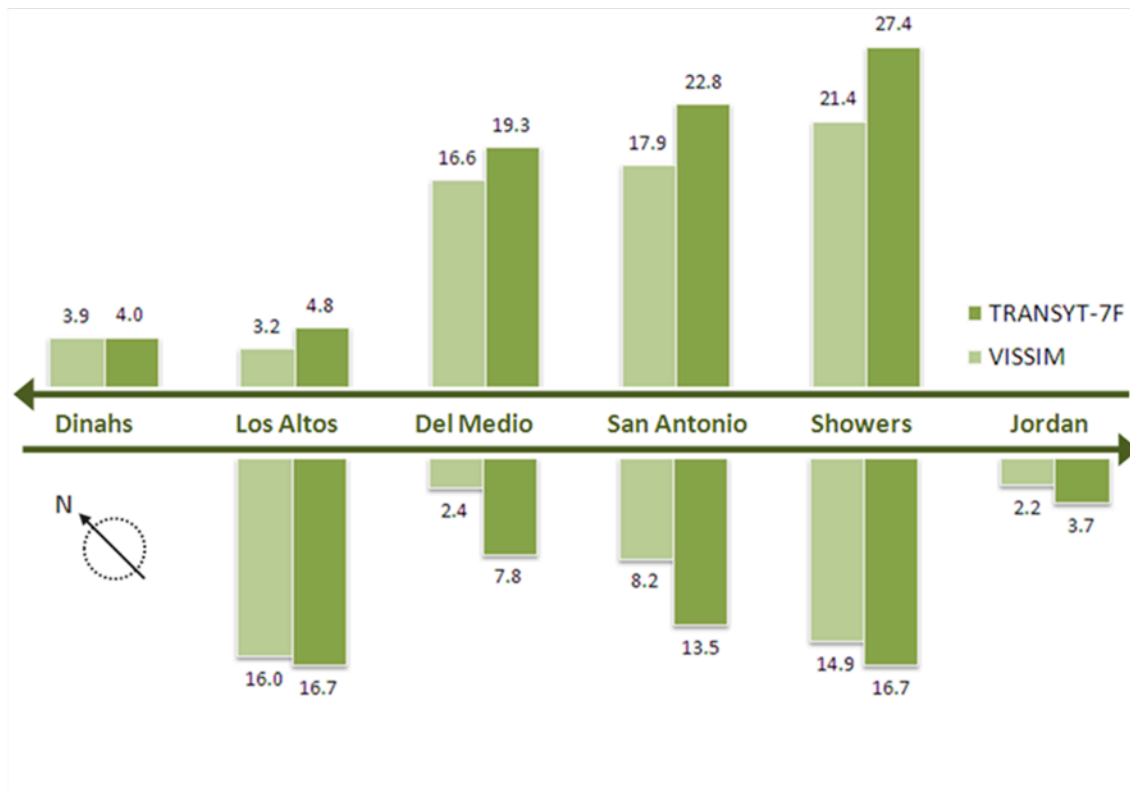


Figure 4-11 Delay per Link for the Current Offsets

As the purpose of the VISSIM simulation is to validate the findings obtained from the offsets optimization model, one should focus on the changes in delay and yellow arrival flow as the results of shifting the offsets. It is reasonable to have a difference in the absolute values obtained by the two simulation models as the simulation environments are different, e.g., fixed-timing versus semi-actuated, and macroscopic versus microscopic. The similarity in the distributions of link flow and link delay demonstrates that this is a valid comparison.

Table 4-3 compares the changes in the total corridor delay and yellow arrival flow as a result of shifting the offsets for TRANSYT-7F model and VISSIM model. With the optimal offsets, the yellow arrival flow is reduced by 49.5 percent in the VISSIM model and by 46.5 percent

in the TRANSYT-7F model; the delay was reduced by 2.5 percent in the VISSIM model as opposed to 4.9 percent in the TRANSYT-7F model.

Table 4-3 Comparison of TRANSYT-7F and VISSIM

Offsets	Corridor Delay (vehicle-hours/hour)		Yellow Arrival Flow (vehicles per hour)	
	TRANSYT-7F	VISSIM	TRANSYT-7F	VISSIM
Current	57.0	41.5	622	253
Optimal	54.2	40.5	354	127
% Change	-4.9%	-2.5%	-46.5%	-49.5%

The same trend shown by the two simulation models, i.e., significant reduction in yellow arrival flow and minor change in delay, demonstrates that the improvement in safety can be achieved without compromising the road efficiency. The offsets optimization model developed under this project is capable of achieving this goal. More significant benefits could be obtained if the safety measures, e.g., the yellow arrival flow, are included in the multiple objective functions in the modern traffic control software/model.

4.5 References

- [4-1] Papageorgiou, M., Diakaki, C., Dinopoulou, V., Kotsialos, A., and Wang, Y., Review of Road Traffic Control Strategies (Contributed Paper). *Proceedings of IEEE*. Vol. 91, 2003.
- [4-2] *VISSIM User Manual, version 3.7*. PTV. Karlsruhe, Germany, April 2003.

5 ACTIVE RED-LIGHT-RUNNING COLLISION AVOIDANCE COUNTERMEASURES

5.1 Introduction

In Chapter 3 of this report, a safety enhanced model was presented. This model is intended to reduce RLR occurrences without compromising the traffic operational efficiency by optimizing the offsets of a coordinated corridor. Optimization gives the best possible solution for a given configuration of traffic. However, the configuration is changing constantly in real traffic, especially due to variation of the behaviors of individual drivers at signalized intersections. We believe that active RLR collision avoidance countermeasures would adapt to traffic better than an off-line optimization method.

Existing research and practices of active RLR collision avoidance countermeasures mainly focus on the dilemma zone protection (e.g., [5-1]). Under the dilemma zone theory, a driver needs to make the stop-or-go decision at the onset of yellow phase, based on his (her) speed (V), distance to the stopline (X), and the yellow duration. If the driver chooses to have a smooth stop, the following kinematics must be satisfied in order to be stopped before the stopline:

$$X \geq X_c = V\delta + \frac{V^2}{2A} \quad \text{Eq. 5-1}$$

where X_c is the critical (minimum) stopping distance, δ is the driver perception/reaction time, and A is the smooth deceleration. If going through is chosen instead, the following

equation must be satisfied in order for the vehicle to arrive at the stopline before the end of the yellow phase:

$$X \leq X_0 = VY \quad \text{Eq. 5-2}$$

where Y is the yellow duration and X_0 is the maximum distance from the stopline for a safe pass through movement. In the situation where $X_0 < X < X_c$, the driver would be in the dilemma zone, in which he (she) can either stop safely after the onset of yellow indication or be able to enter the intersection before the ends of the yellow indication. Figure 5-1 graphically illustrates the dilemma zone at an intersection and Figure 5-2 shows the dilemma zone in the X-V diagram.

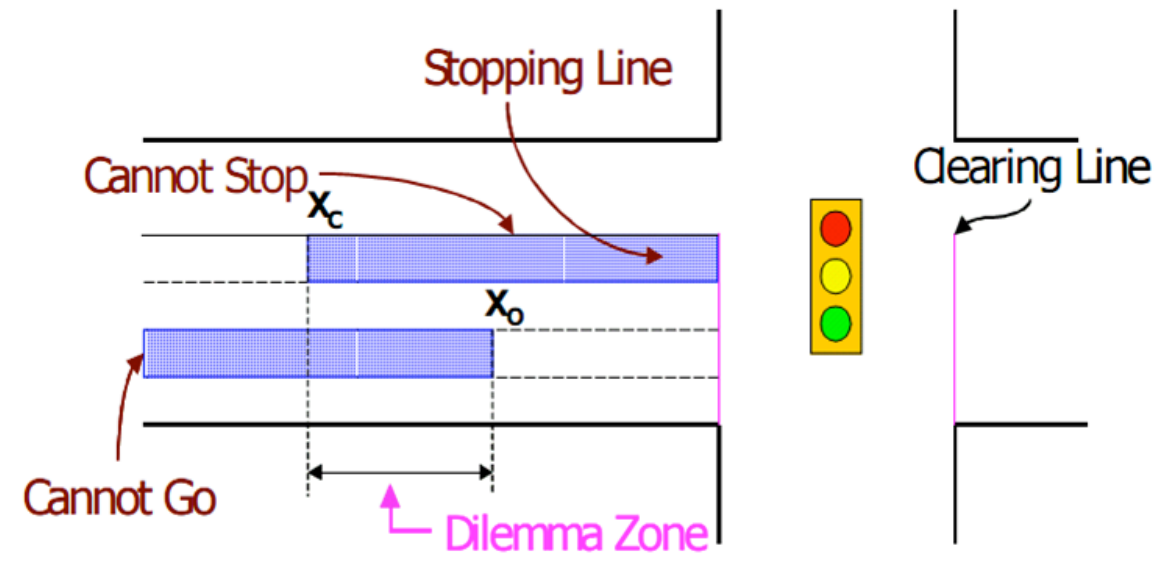


Figure 5-1 Dilemma Zone (taken from [5-4])

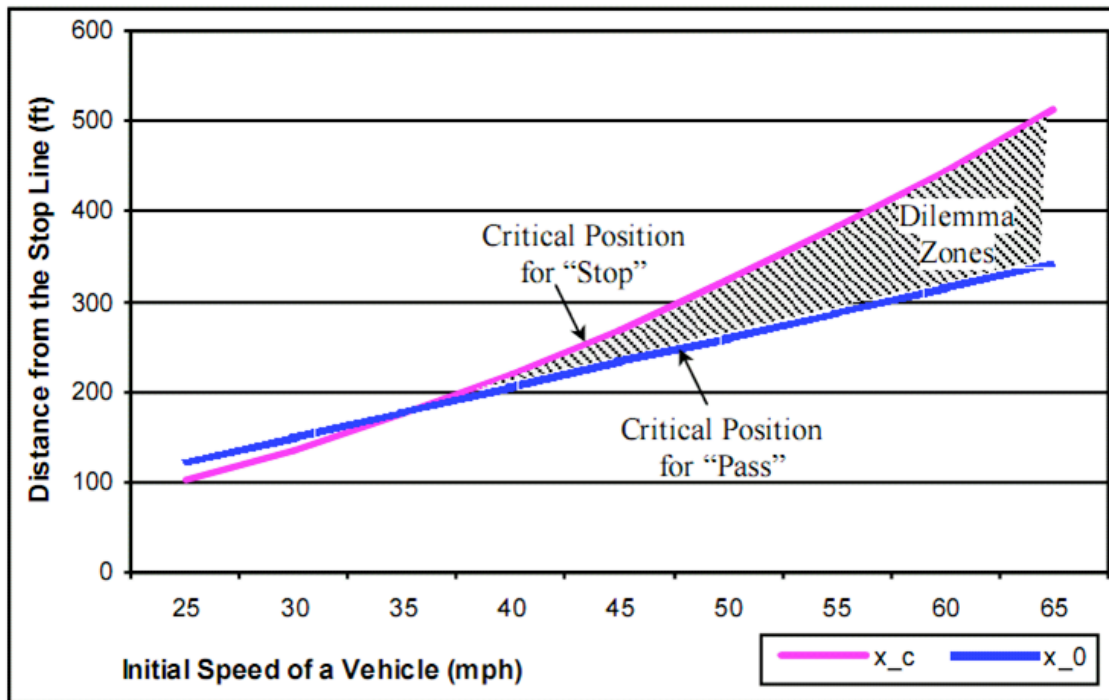


Figure 5-2 Distance to Stopline – Speed Diagram of Dilemma Zone (taken from [5-4])

Several dilemma zone protection systems, also referred as the green extension systems, have been developed (e.g., [5-2]). The idea behind such systems is to extend the green phase if a vehicle is being detected or predicted in the dilemma zone.

The Detection Control System (D-CS) developed by Texas Transportation Institute ([5-3]) is an extension of the dilemma zone protection systems, which uses additional strategies to allow the truncation of the green phase. In the D-CS system, the determination of the termination point for the green phase is formulated as a minimization problem, with the objective function as the number of vehicles in dilemma zone.

Three major assumptions are used for the dilemma zone protection systems:

- Drivers being caught in the dilemma zone is an substantial causal factor of RLR and related collisions;
- Drivers make stop-or-go decisions at the onset of yellow and will maintain the decision during the yellow interval; and
- The predefined driver behavior related parameters, including the perception/reaction time (δ) and the acceptable deceleration (A), represent the majority of the motorists.

Liu et al. ([5-5]) investigated the responses of drivers when approaching intersections with a yellow indication, with more than 1,000 observations at six intersections. They found that the observed drivers' stop-or-go decisions are substantially different than what is described by the dilemma zone theory, due to the variations in the behavior of driving populations, and that the green extension may not eliminate all dilemma zones.

As presented in Chapter 2, our empirical data analysis showed that the yellow arrival flow can potentially be a safety measure and it has been used in the development of the offline offsets optimization model. Efforts have been devoted to extend this concept in the development of active RLR countermeasures. These efforts are presented in the following sections.

5.2 Active Offsets Refining

A reasonable extension of the offline offsets optimization is to make it adaptive to changes in traffic flows. The controllers use time-of-day plans to account for traffic changes during the day. The same time-of-day plan could be in place for several hours regardless of changes in

traffic demands during this period. The offline optimization provides the best possible offsets for the given average or maximum traffic demand during the several-hour period. However, the real traffic demands vary during the same period. As a consequence, the offline offsets may not be optimal at some times. Developing a mechanism that adapts to real traffic demands could further improve the intersection safety.

A feasibility study was performed to evaluate the effectiveness of this approach. The flows that were used for the development of the offline offsets model is treated as the base line and the variances in flows are presented as 98%, 90%, and 70% of the base line. The optimal offsets correspond to different flows are obtained using the optimization tool, with the same weight and control variables (cycle length, green splits, and phase sequence). The results are presented in Table 5-1 and graphically illustrated in Figure 5-3.

Table 5-1 Evaluation of the Active Offsets Refining Approach

Flow	Delay (vehicle-hours per hour)			Yellow Arrival Flow (vehicles per second)		
	Current	Optimal	% change	Current	Optimal	% change
100%	56.9	53.7	-5.6%	6.0	3.5	-42%
98%	55.9	52.9	-5.4%	5.8	3.3	-43%
90%	49.2	46.8	-4.9%	5.4	3.1	-43%
70%	36.0	34.6	-3.9%	4.0	1.9	-53%

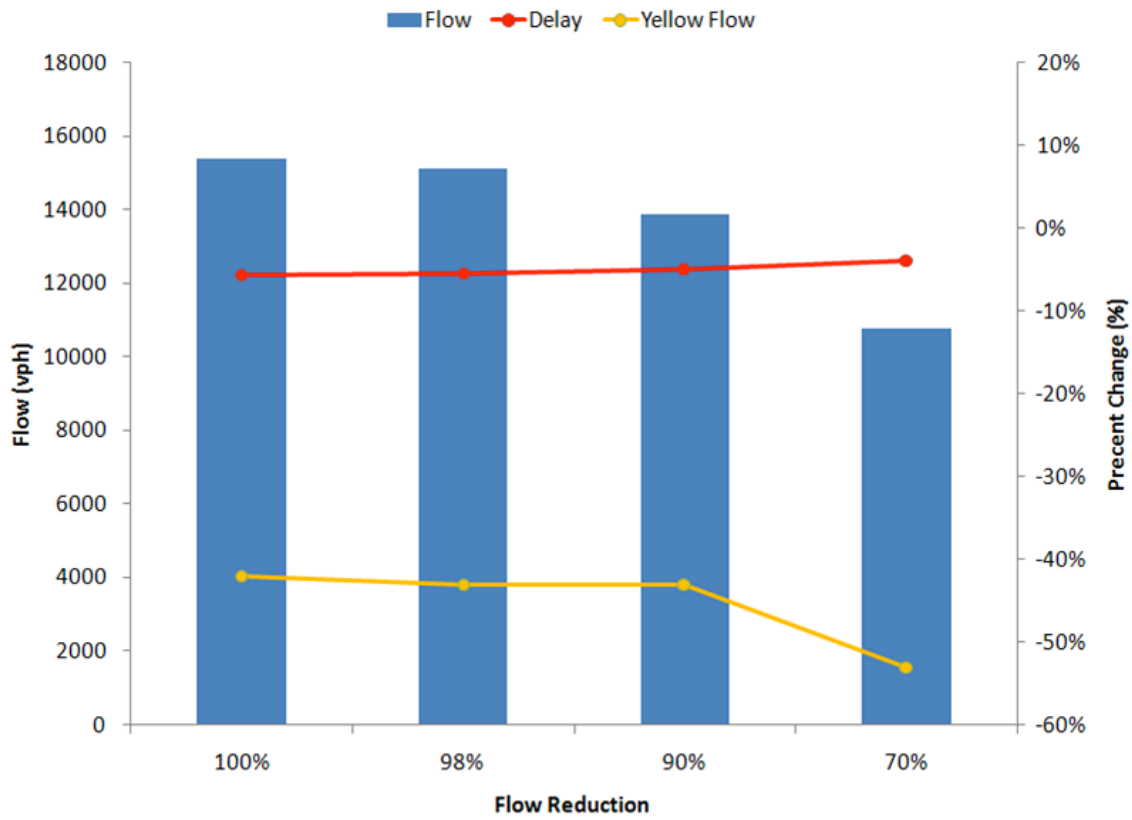


Figure 5-3 Evaluation of the Active Offsets Refining Approach

As can be seen, when reducing flows, the effectiveness of yellow flow reduction improved from 42 percent reduction to 53 percent reduction and the changes in delay remained minor, from 5.6 percent reduction to 3.9 percent reduction. The results demonstrate the potential of this approach in improved intersection safety.

5.3 Dynamic Yellow Onset

Another countermeasure that derives from the relationship between the yellow arrival flow and the RLR occurrences is the dynamic yellow onset. The dynamic yellow on-set determines the “best” point to terminate the green phase around the default onset of the yellow phase in

order to minimize the probability of RLR collision. This can be formulated as a minimization problem as follows:

We assume that a continuous vehicle detection means or a series of discrete point detectors can detect vehicle's speed (v), distance to the stopline (x), and the occupied lane on an approaching link. The detection range covers the travel time T_0 seconds to the stopline. We also assume t_Y is the default onset of the yellow phase and T is the upper bound for truncating or extending the green phase. The problem of dynamic yellow onset is to find the best point $\tau \in [t_Y - T, t_Y + T]$, to terminate the green phase so that the probability of collision is minimized.

At the current time t , we can sort the N approaching vehicles based on their occupied lane J , and their distances to the stopline, i.e.,

$$SV_J = \{(x_i, v_i) | 0 < x_1 < x_2 < \dots < x_N\} \quad \text{Eq. 5-3}$$

Given an empirical probability density function of stopping, P_S , under the condition that the vehicle state (x, v) at the onset of yellow (the selection of P_S is presented in the following chapter), there is a probability of stopping associated with each vehicle in SV_J , i.e., $P_S^i(t)$, $i = 1, \dots, N$. The probability of going through for vehicle j in SV_J is then given by

$$P_G^j(t) = \prod_{i=1}^j (1 - P_S^i) \quad j = 1, \dots, N \quad \text{Eq. 5-4}$$

and its associated time-to-cross the stopline with respect to the onset of the red phase is given by

$$T_C^j(t) = \min(0, T2I_j - Y) \quad j = 1, \dots, N \quad \text{Eq. 5-5}$$

where $T2I = \frac{x}{v}$ is the time-to-intersection and Y is the yellow interval.

By projecting vehicles states, assuming the drivers maintain their speed before the onset of yellow, one can obtain $P_G^j(\tau)$ and $T_C^j(\tau)$ at the potential ends of the green phase, τ . As the risk of collision is higher if a vehicle enters the intersection later in red, one objective function associated with the probability of collision could be the expectation value of the violation time into red, given by

$$\text{Risk}(\tau) = E[T_C] = \sum_j P_G^j(\tau) \cdot T_C^j(\tau) \quad \text{Eq. 5-6}$$

while another objective function could be the maximum possible violation time into red, given by

$$\text{Risk}(\tau) = \max_j (T_C^j(\tau)) \quad \text{Eq. 5-7}$$

The best green end point or the onset of yellow is then determined by

$$\min_{\tau} \text{Risk}(\tau) \quad \text{Eq. 5-8}$$

5.4 Dynamic Red Clearance Interval

Several studies have investigated the amount of time after the onset of the red phase that red-light violators enter an intersection (e.g., [5-6]). They all reported that the red-light violation frequency decreases as the violation time into red increases and the majority of violations occur within the first a couple of seconds in red.

We collected red-light camera recorded violation incident data at 23 photo-enforced intersections from San Francisco Department of Parking and Transportation (DPT). A total of 2,869 red-light violations occurred in the month of June 1998.

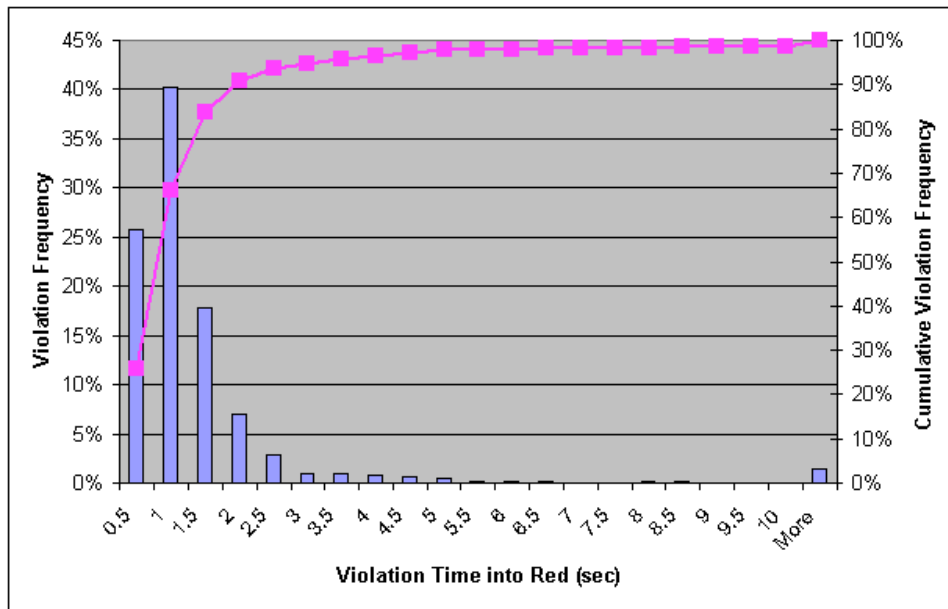


Figure 5-4 Red-Light Violation Frequency versus Violation Time into Red

Figure 5-4 shows the relationship of violation frequency and violation time into red. Among all violations, about 66 percent of drivers entered the intersection within 1 second after the

start of red and another 25 percent of drivers entered the intersection within 1 and 2 seconds into red. This result roughly agrees with other studies.

The red clearance interval has been implemented by many traffic agencies for the purpose of reducing RLR collisions. It provides clearance time for vehicles which have entered an intersection prior to conflicting movements receive a green indication. Given that most of red-light violators entered the intersection within a few seconds after the start of red, implementing the red clearance interval has a great potential to reduce the number of collisions resulting from these violations.

Souleyrette et al. ([5-7]) studied the effectiveness of red clearance interval in reducing intersection collisions. The study reported that a reduction in collisions occurred in the year immediately following the implementation of the red clearance interval. However, the number of collisions went up after the first year and no long term benefits were observed. The results demonstrate that: (1) implementing a red clearance interval has the potential to reduce intersection collisions and (2) using a fixed red clearance interval has limitations because drivers who try to take advantage of the clearance time could cause collisions. We believe that dynamic red clearance interval will perform better than a fixed clearance interval because, by definition, it only extends the red clearance interval when it is needed to reduce a potential collision and therefore, drivers would not be likely to perceive the change.

Two functional elements are required for the dynamic red clearance interval approach: (1) the prediction of RLR and related collision; and (2) the estimation of the red clearance interval. To develop algorithms to predict the probability of a conflict, driver behaviors when approaching an intersection during the signal phase transition and when entering an intersection after the starts of green need to be investigated.

5.5 References

- [5-1] Papaioannou, P., Driver Behavior, Dilemma Zone and Safety Effects at Urban Signalized Intersections in Greece. *Accident Analysis and Prevention*. Vol. 39, 2007.
- [5-2] Pant, P. D., Cheng, Y., Rajagopai, A., and Kashayi, N., *Field Testing and Implementation of Dilemma Zone Protection and Signal Coordination at Closely-Spaced High-Speed Intersections*. Report No. FHWA/OH-2005/006. Washington, DC: Federal Highway Administration, May 2005.
- [5-3] Bonneson, J., Middleton, D., Zimmerman K., Charara, H., and Abbas, M., *Intelligent Detection-Control System for Rural Signalized Intersections*. Report No. FHWA/TX-03/4022-2. Washington, DC: Federal Highway Administration, August 2002.
- [5-4] Chang, G.-L., Xiang, H., and Chou, C.-S., *Interrelations between Crash Rates, Signal Yellow Times, and Vehicle Performance Characteristics*. Report No. MD-04-SP. University of Maryland, College Park. June 2004.
- [5-5] Liu, Y., Chang, G.-L., Tao, R., Hicks, T., and Tabacek, E., Empirical Observations of Dynamic Dilemma Zones at Signalized Intersections. *In Proceedings of TRB 86th Annual Meeting*. Transportation Research Board, Washington DC, January 2007.
- [5-6] Bonneson, J. A., Zimmeman, K., and Bewwer, M., *Engineering Countermeasures to Reduce Red-Light-Running*. Report No. FHWA/TX-03/4027-2. Washinton DC: Federal Highway Administration. August 2002.

[5-7] Souleyrette, R., O'Brien M., McDonald, T., Preston, H., and Storm, R.,
Effectiveness of All-Red Clearance Interval on Intersection Crashes. Report No. MN/RC-
2004-26. FHWA/TX-03/4027-2. Minnesota Department of Transportation. May 2004.

6 STUDY DRIVERS DECISION MAKING AT SIGNALIZED INTERSECTIONS

6.1 Introduction

Many factors affect drivers' stop-or-go decision when approaching an intersection and encountering a yellow signal indication. The success of a RLR collision avoidance system relies on the capability and the accuracy in detecting and predicting RLR. In [6-1], it was reported that it is possible to use speed to separate running-through vehicles from stopping vehicles (Figure 6-1). On an approach with the speed limit as 40 mph, the potential separation point could be at 150 feet (46 meters) upstream of the intersection (the 100 ft mark in Figure 6-1), where all the through motorists are traveling above 28 mph and all the stopping motorists are traveling below 28 mph.

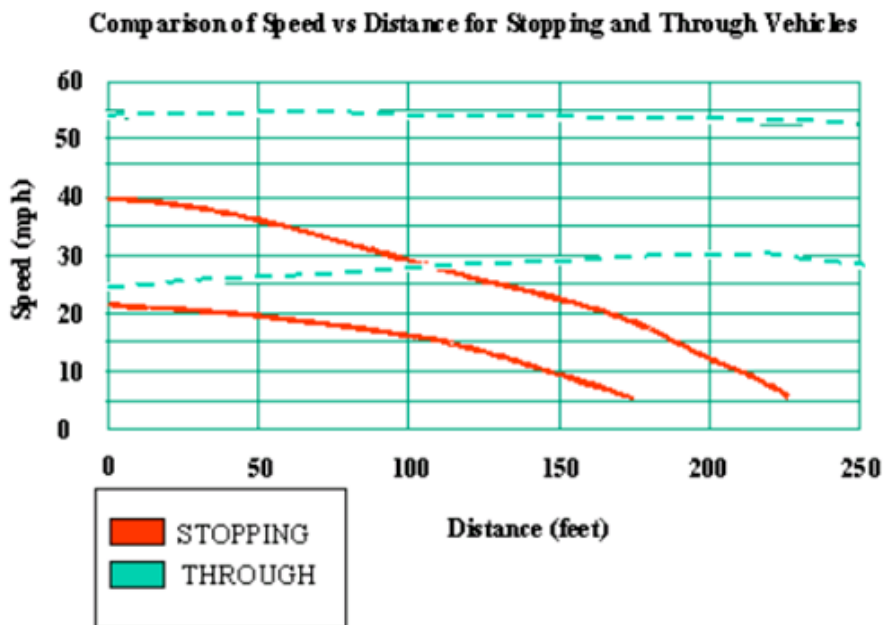


Figure 6-1 Different Characteristics of Stopping and Through Vehicles

However, the travel time from the separation point to the stopline, if traveling at the speed limit, is about 2.5 seconds, which is less than the yellow duration. This potential separation point is less than the necessary distance needed to capture drivers' response to the yellow onset. Furthermore, the data samples also include non-RLR-related samples, such as vehicles that crossed the stopline during green and those stopped behind the first stopping vehicle.

The most common variables used in studying drivers' stop-or-go decision at the onset of the yellow indication include the distance to the stopline, the travel time to the stopline, or a combination of these two variables. Goh and Wang ([6-2]) reported that the measures could be different with respect to drivers' states at the yellow onset, distance dominated when near the stopline, time dominated when in the intermediary, and speed dominated when further away from the stopline.

In the attempt to develop algorithms to predict RLR, we installed pneumatic road tubes at the intersection of 28th Avenue crossing El Camino Real, San Mateo, California. The findings are presented in the following sections.

6.2 Data Collection

Speeds for individual vehicles were collected at 5 locations on the curb lane of the northbound direction, as shown in Figure 6-2. Table 6-1 lists the locations of the speed measurements.

Table 6-1 Locations of Speed Tubes

Detector ID	Distance to Stopline (m)
1	106
2	61
3	30
4	-5
5	-17



Figure 6-2 Data Collection Site

In addition to the speed data, signal status data were also collected.

6.3 Data Association to Reconstruct Vehicle Trajectories

A simple nearest-neighbor data association algorithm was developed to reconstruct vehicle trajectories from the anchor points. Given two sets of speed measurement $\{(t_I, v_I)\}$ and $\{(t_{II}, v_{II})\}$ at two locations with distance to the stopline as x_I and x_{II} , the following kinematics equation should be satisfied if the vehicle is traveling with a constant acceleration, a , crossing the two points:

$$\begin{aligned}v_{II} &= v_I + a \cdot (t_{II} - t_I) \\x_I &= x_{II} + v_I \cdot (t_{II} - t_I) + \frac{a}{2} (t_{II} - t_I)^2\end{aligned}\tag{Eq. 6-1}$$

hence

$$x_I = x_{II} + \frac{v_I + v_{II}}{2} (t_{II} - t_I)\tag{Eq. 6-2}$$

Define

$$f = \frac{v_I + v_{II}}{2} (t_{II} - t_I) - (x_{II} - x_I)\tag{Eq. 6-3}$$

Given a sample measure of (t_I, v_I) , the data association is to find the corresponding sample in $\{(t_{II}, v_{II})\}$ so that it minimizes f .

Applying the method described above, a total of 4,885 vehicle trajectories were reconstructed and synchronized with the signal status (464 cycles). Of those, 152 relevant trajectories were selected for this study. A relevant trajectory is defined as the detected vehicle either crossed the stopline during the yellow or red indication or was the first stopping vehicle. Figure 6-3 illustrates the relevant vehicle trajectories. The horizontal axis is the distance to the stopline in

meters and the vertical axis is vehicle's speed in meters per second. Among the 152 trajectories, 44 are from the first stopped vehicle (blue color in Figure 6-3), 84 are from vehicles that crossed the stopline during the yellow (yellow color in Figure 6-3), and 24 are RLR occurrences (red color in Figure 6-3). Figure 6-4 shows RLR frequency versus the entering time into red. 92 percent of RLR occurrences entered the intersection within 2 seconds after the start of red.

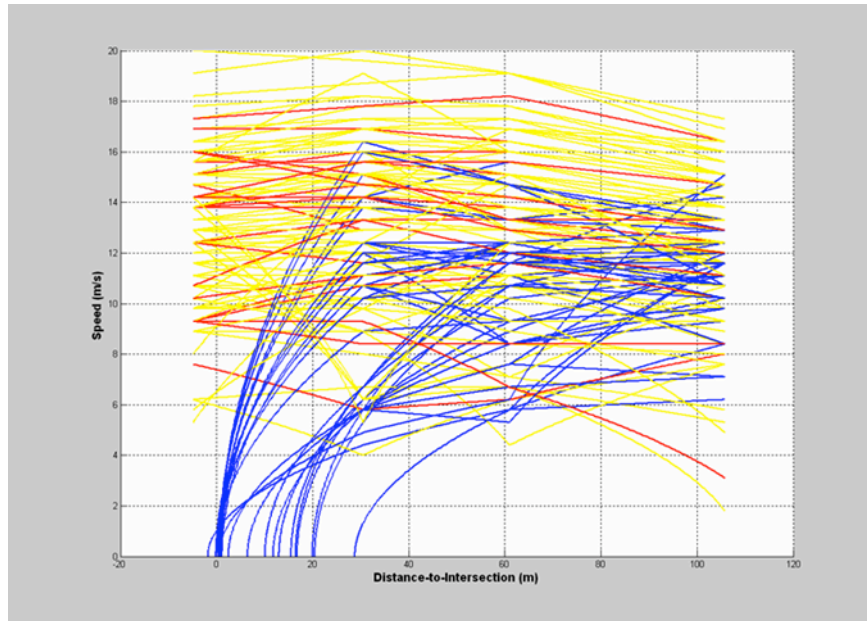


Figure 6-3 Reconstructed Vehicle Trajectories

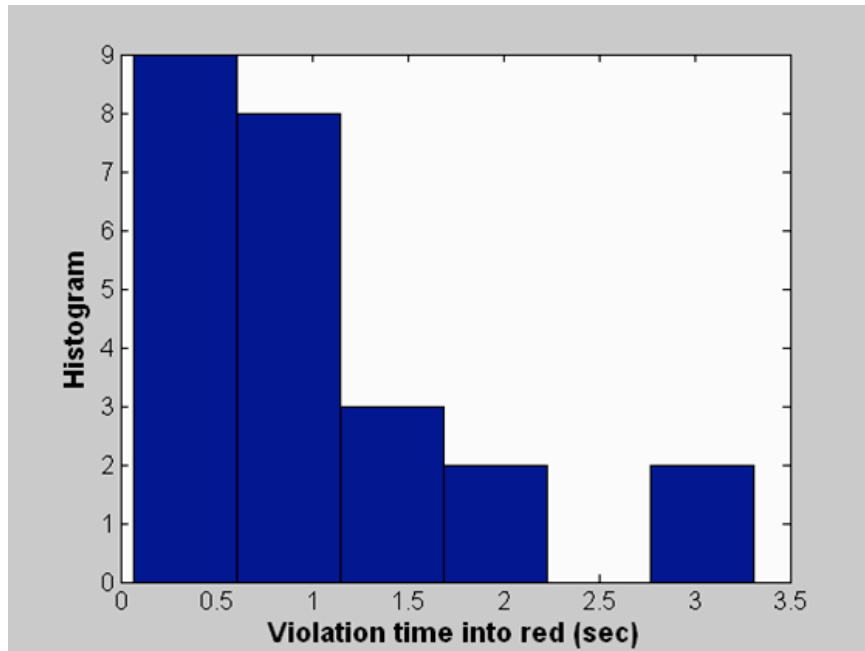


Figure 6-4 RLR Frequency versus Entering Time into Red

Figure 6-5 shows the relationship between the percentage of vehicles stopped and the travel time to the stopline. It clearly shows the probability of stopping before the stopline increases significantly when the travel time to the stopline is greater than 5 seconds.

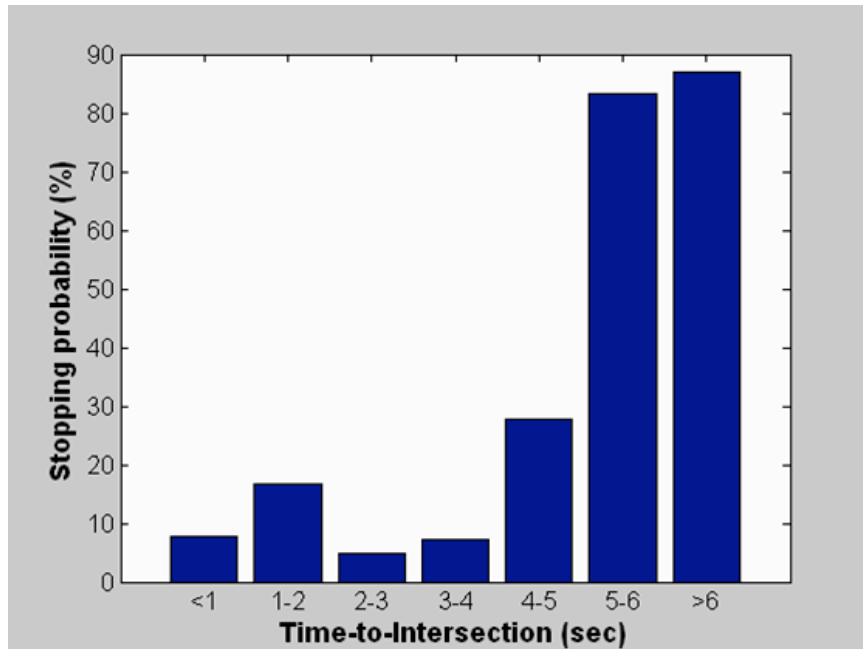


Figure 6-5 Stopping Probability versus Travel Time to the Stopline

6.4 Prediction of Red-Light Running

Logistic regression was chosen for modeling the probability of stopping, i.e.

$$p_s(x) = \frac{1}{1 + e^{-(a+b^T x)}} \quad \text{Eq. 6-4}$$

where x is the dependent variables, a combination of vehicle states, b is the estimated parameter vector, and a is the regression constant. At the yellow onset, the “best” combination of variables is speed, acceleration, and the product of distance and speed, as shown in Table 6-2.

Table 6-2 Parameters Estimated at Yellow Onset

Variables in the Equation

		B	S.E.	Wald	df	Sig.	Exp(B)
Step 1	V	-1.202	.245	24.006	1	.000	.301
	DV	.011	.002	24.065	1	.000	1.011
	A	-1.850	.526	12.382	1	.000	.157
	Constant	5.239	1.608	10.616	1	.001	188.472

a. Variable(s) entered on step 1: V, DV, A.

The outcome of Eq. (6-4) is then used to predict RLR, i.e., RLR likely occurs if the probability of stopping is less than 0.5 and the estimated travel time to the stopline is after the start of red. The travel time to the stopline is estimated by assuming the vehicle will maintain its speed and acceleration. Table 6-3 illustrates the performance in predicting RLR with respect to different groups of trajectories. The overall prediction accuracy is as high as 92 percent.

Table 6-3 Performance in Predicting RLR at Yellow Onset

Observed Behavior	Number of Observations	Prediction		
		Stopping	Through in Yellow	RLR
Stopped	44	38	0	6
Through during Yellow	84	1	82	1
RLR	24	3	1	20

As mentioned in section 5.3, an empirical data based probability of stopping is required for the countermeasure of dynamic yellow onset. The model described above could serve this purpose.

However, for the countermeasure of dynamic red clearance interval, predicting RLR during the yellow phase would achieve higher correct prediction rate as more information about drivers' response to the yellow indication is available. Logistic regression was performed for

the time to the onset of red (T2R) at 3, 2 and 1 second, respectively, and the performance in predicting RLR is presented in Table 6-4. The correct prediction rate increases as the prediction is made further towards the end of yellow, as shown in Figure 6-6.

Table 6-4 Performance in Predicting RLR during the Yellow Phase

T2R (sec)	Observed Behavior	Number of Observations	Prediction		
			Stopping	Through in Yellow	RLR
4	Stopped	44	38	0	6
	Through during Yellow	84	1	82	1
	RLR	24	3	1	20
3	Stopped	40	34	0	6
	Through during Yellow	70	0	70	0
	RLR	24	3	0	20
2	Stopped	36	32	0	4
	Through during Yellow	48	0	48	0
	RLR	24	3	0	21
1	Stopped	34	33	0	1
	Through during Yellow	31	0	31	0
	RLR	24	2	0	22

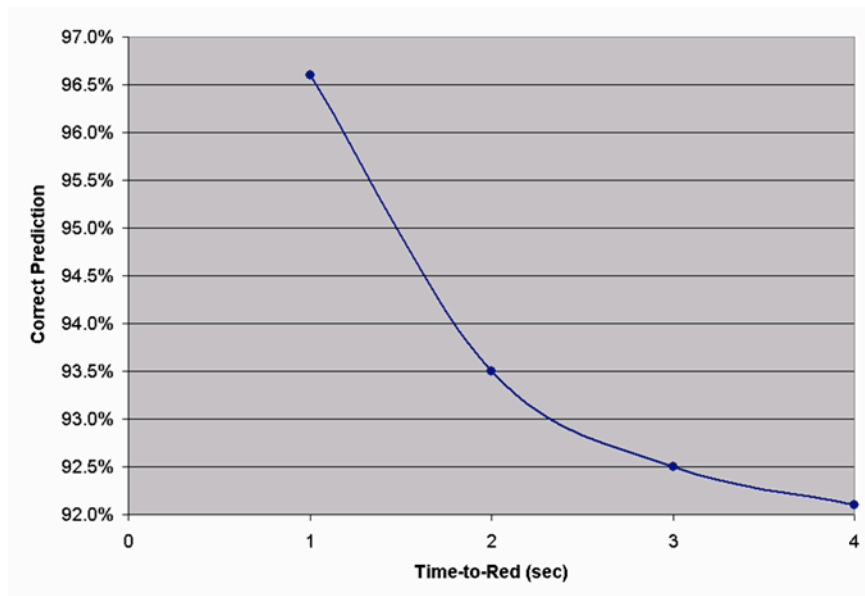


Figure 6-6 Correct RLR Prediction Rates

6.5 Drivers' Situation Zones

In order to further improve the accuracy in predicting RLR, we investigated how drivers' situation zones relate to RLR. The situation zones are defined based on the required deceleration rate for a stop and the travel time to the stopline with respect to the remaining time in yellow, as illustrated in Figure 6-7.

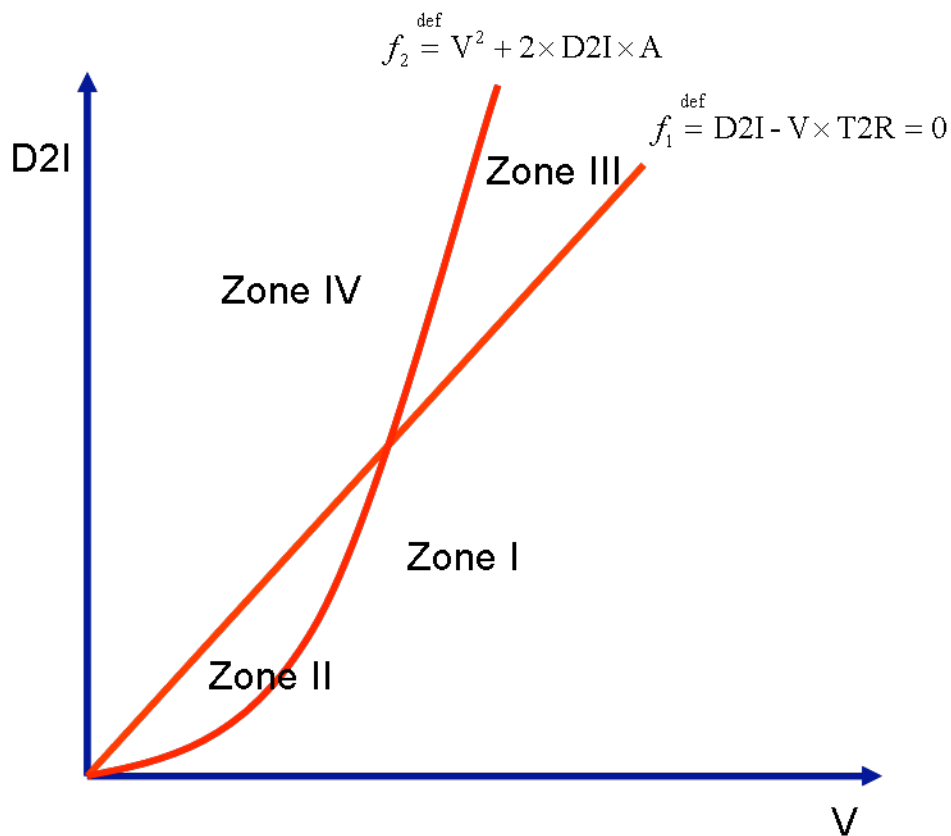


Figure 6-7 Drivers' Situation Zone with a Yellow Indication

Drivers in Zone I may enter the intersection before the start of red indication if they maintain the current speed. Drivers in Zone II may either enter the intersection before the start of red if maintaining the current speed or stop with the current deceleration. Drivers in Zone III need

either to speed up in order to enter the intersection before red or decelerate to a stop. And drivers in Zone IV can stop with the current deceleration.

Based on the situation zone that he (she) was in and the observed stop-versus-go decision, drivers can be classified into 4 groups: conservative, normal, aggressive, and not-certain, as illustrated in Table 6-5.

Table 6-5 Classification of Drivers

Zone	Observed Decision	
	Stop	GO
I ($f1 < 0, f2 > 0$)	Conservative	Normal
II ($f1 < 0, f2 < 0$)	Conservative	Normal
III ($f1 > 0, f2 > 0$)	Not-Certain	Not-Certain
IV ($f1 > 0, f2 < 0$)	Normal	Aggressive

Table 6-6 summarizes drivers' situation zones versus the decision made during the yellow phase.

Table 6-6 Drivers' Situation Zones during the Yellow Indication

T2R (sec)	Observed Behavior	Number of Observations	Situation Zones			
			I	II	III	IV
4	Stopped	44	2	5	25	12
	Through during Yellow	84	79	0	4	1
	RLR	24	0	0	24	0
3	Stopped	40	2	3	25	10
	Through during Yellow	70	67	0	3	0
	RLR	24	0	0	24	0
2	Stopped	36	0	2	22	12
	Through during Yellow	48	47	0	1	0
	RLR	24	0	0	24	0
1	Stopped	34	0	0	18	16
	Through during Yellow	31	31	0	0	0
	RLR	24	0	0	24	0

Several observations can be made from Table 6-6:

- Aggressive and conservative drivers respond to the yellow indication earlier than average drivers;
- The majority of decisions were made during the first 2 seconds of yellow, and drivers seem not change their decision in the last 2 seconds of yellow;
- Red-light runners were always in zone III; and
- Sometimes stopped drivers apply brakes only during the last couple of seconds of yellow, although they might have decided to stop earlier.

It clearly showed that the prediction of RLR should focus more on drivers in Zone III at 2 seconds to the start of red. Logistics regression was then performed for Zone III drivers only.

The “best” variable found is $f_1^{\text{def}} = D2I - V \cdot T2R$ (Table 6-7), where D2I is the distance to the stopline, v is the speed, and T2R is the time to the onset of red.

Table 6-7 Parameters Estimated for Zone III

		Variables in the Equation					
		B	S.E.	Wald	df	Sig.	Exp(B)
Step	D by f1	.195	.059	11.060	1	.001	1.215
1	Constant	-4.342	1.315	10.897	1	.001	.013

a. Variable(s) entered on step 1: D * f1 .

The correct RLR prediction rate increased from 93.5 percent when a single model is used on all vehicles to 94.4 percent when different models are applied on different groups of drivers.

It is necessary to point out that the results from this study are based on limited samples. It is essential to validate these findings with larger samples.

6.6 References

[6-1] Bellomo-McGee Incorporated. *Intersection Collision Avoidance Study, Final Report*. Federal Highway Administration. September 2003.

[6-2] Goh, P. K. and Wong, Y. D., *Effects of distance and speed on driver stop-versus-cross at traffic signals*. Road and Transportation Research, ARRB Transportation Research Ltd, Australia. Vol. 13, September 2004.

7 CONCLUSIONS AND NEXT STEPS

There is no doubt that unsafe driving could cause red-light-running crashes, injuries and fatalities. Driver education and automated red-light enforcement systems can effectively reduce red-light-running crashes caused by unsafe driving. However, there are other factors that contribute to red-light-running crashes. For those factors, engineering countermeasures that change the intersection environment may be more effective in improving intersection safety than education and enforcement, which aim to change the intersection users.

Under this project, efforts have been made towards this direction. Using second-by-second signal phasing and interval data together with loop data, our cycle-based data analysis showed that traffic flow arriving at the intersection during the yellow phase has the largest impact on RLR occurrences. The significance of this finding is that yellow arrival flow is controllable through signal timing adjustment. We developed a signal synchronization algorithm that takes the yellow arrivals into consideration in the design of signal offsets. We demonstrate the effectiveness of signal synchronization in both microscopic simulation and macroscopic simulation environments. Simulation results showed the benefits of synchronization: yellow arrivals were significantly reduced without compromising intersection efficiency. More significant benefits could be obtained if the yellow arrival flow is included in the multiple objective functions in the modern traffic control software.

The designed signal offset is optimal with a given configuration such as traffic flows and densities. However, the configuration is constantly changing in real traffic and as a result the designed offset is no longer optimal. We simulated an active offset refining scheme that

adjusts signal offset based on traffic flow fluctuation. The results demonstrate the potential of this approach in improved intersection safety.

The design of signal offsets focus on the macroscopic flow level. Red-light-running crashes may relate more with the behavior of individual drivers. The future research direction to reduce the probability of RLR, following the concept of controlling the yellow arrival, would be to adaptively adjust the onset of yellow based on vehicle arrival patterns. We studied drivers' decision making when approaching an intersection during the phase transition using collected real world data and developed a model to predict the probability of RLR for individual drivers. We acknowledge the fact that the result is based on limited data and it is a preliminary effort towards future research.